BMR Journal of Australian Geology & Geophysics, 12, 3, 223–244

Differentiation of Late Cambrian–Early Ordovician species of *Cordylodus* (Conodonta) with biapical basal cavities

Robert S. Nicoll[1]

Four species of the conodont genus *Cordylodus* are recognised, containing elements that have two apices in the basal cavity (biapical), one extending into the cusp and the other into the first denticle of the posterior process. They are *C. prion* Lindström 1955, *C. lindstromi* Druce & Jones, 1971, *C. prolindstromi* sp. nov. and *C. sp. nov. B. Cordylodus* sp. nov. B has been found only in a single sample and insufficient material is available to establish limits of element morphological variability. In the Ninmaroo Formation of the Georgina Basin, northern Australia, *C. prolindstromi* sp. nov. is found stratigraphically below the first occurrence of *C. lindstromi*. This relationship may be important in the resolution of the placement of the Cambrian–Ordovician boundary. In all four species, the biapical cavity is best developed in the S elements, poorly developed in the P elements and, except in *C. prion*, absent in the M element. Multiple basal cavity apices that extend into the cusp and into the base of one or more denticles of the posterior process, may be found in aberrant specimens of most species of *Cordylodus*, but the consistent presence of the biapical cavity seems to be limited to these four species of the genus. There has been some confusion in the literature about the application of the name *Cordylodus lindstromi* and most previous identifications of *C. lindstromi* now need re-evaluation in the light of the species definitions established here.

Introduction

The interpretation of species of the conodont genus *Cordylodus* with two apices in the basal cavity, the primary extending into the cusp and the secondary into the first denticle of the posterior process, has caused much taxonomic and biostratigraphic confusion. Most of these biapical specimens have either been assigned to *Cordylodus lindstromi* Druce & Jones or been considered aberrant specimens of a form normally having only a single apex to the basal cavity (Landing & others, 1980). However, Nicoll (1990) examined type and topotype material of *C. lindstromi* from the Ninmaroo Formation (Georgina Basin, western Queensland) and comparative material from the Wilberns Formation (Texas). He concluded that a morphologically distinct species, with a full septimembrate apparatus, could be recognised. Nicoll (1990) also indicated that the 'notched' forms illustrated as *C. lindstromi* by Barnes (1988) and Andres (1988) should be assigned to a new species and that some stratigraphically old elements of *C. lindstromi* had a flattened secondary apex (Nicoll, 1990, table 3).

This paper extends the investigation of biapical basal cavities in *Cordylodus* from *C. lindstromi* to three additional species. Two of these are the notched form, which is *C. prion* Lindström (1955), and the flattened tip form, which is herein named *C. prolindstromi* sp. nov. The accurate differentiation of these three species is critical in the recognition of one of the proposed levels of the Cambrian–Ordovician boundary. The third additional species, *C.* sp. nov. B, has been recovered from a single sample from the upper part of the Ninmaroo Formation, but too few specimens have been found to define the complete apparatus structure.

Several conodont species and faunas have been re-examined recently in investigating the Cambrian–Ordovician boundary (Nicoll, 1990; Nicoll & Shergold, 1991; this study), and some key samples containing species relevant to the understanding of speciation of the genus *Cordylodus* have been examined. These include the Stora Backor sample 5 (Västergötland, Sweden), from the Lindström (1955) study of the Ordovician of central Sweden, and new samples from the Ninmaroo Formation at Black Mountain in western Queensland (Druce & Jones, 1971; Nicoll & Shergold, 1991; Shergold & Nicoll. in press).

[1]Onshore Sedimentary & Petroleum Geology Program, BMR, GPO Box 378, Canberra ACT 2601

Sample 5 from the Lindström (1955) section in the Änga Quarry at Stora Backor contained a new species of *Cordylodus*, *C. prion*, as well as other taxa important to the understanding of Early Ordovician conodont speciation. Lindström (1955) identified 20 form species (subsequently reduced to about 10 multielement taxa) in the sample. Olgun (1987) identified 22 species from the same interval, but many of them are considered here to be reworked Cambrian and earlier Ordovician forms. For this study I analysed a single block of limestone (collected by John Repetski, U.S Geological Survey, Reston, Va) from the nodular bed of Lindström's section diagram (1955, fig. 1). The 822 g sample was processed in buffered acid and sieved using a 75 micron sieve. The residue was subjected to magnetic separation to remove the abundant glauconite. Over 5000 of the better preserved ramiform elements and representative coniform elements were then selected for study.

At the Black Mountain section (Fig. 1) in the Georgina Basin of western Queensland, two sets of samples, one collected by R.L. Ripperdan and J.L. Kirschvink (California Institute of Technology) in 1989 and the second by J.H. Shergold, R.S. Nicoll, J.R. Laurie, B.M. Radke, R.W. Brown (Bureau of Mineral Resources) and A.T. Nielsen (University of Copenhagen) in 1990, have recently been taken through the Chatsworth Limestone and Ninmaroo Formation for biostratigraphic and palaeomagnetic study (Ripperdan & others, 1990, Nicoll & Shergold, 1991). A total of 303 new samples, 65 from the Chatsworth Limestone and 238 from the Ninmaroo Formation, were collected through this 1000 m thick section and have been examined for conodonts. Revisions of the conodont biostratigraphy of the pre-*Cordylodus* interval have been published (Nicoll & Shergold, 1991) and preparation of the fauna from the rest of the section is in progress.

Evolutionary development of Cordylodus

The genus *Cordylodus* can be divided into a root stock and three distinct lineages based on gross morphological differences, especially in the cusp of the P elements. The root stock is the evolutionary lineage of *C. primitivus* Bagnoli & others (1987) — *C. proavus* Müller (1959) — *C. caboti* Bagnoli & others (1987), a group that is structurally simple, but which show increasing morphological complexity. The first branch from this stock consists of species with biapical basal cavities

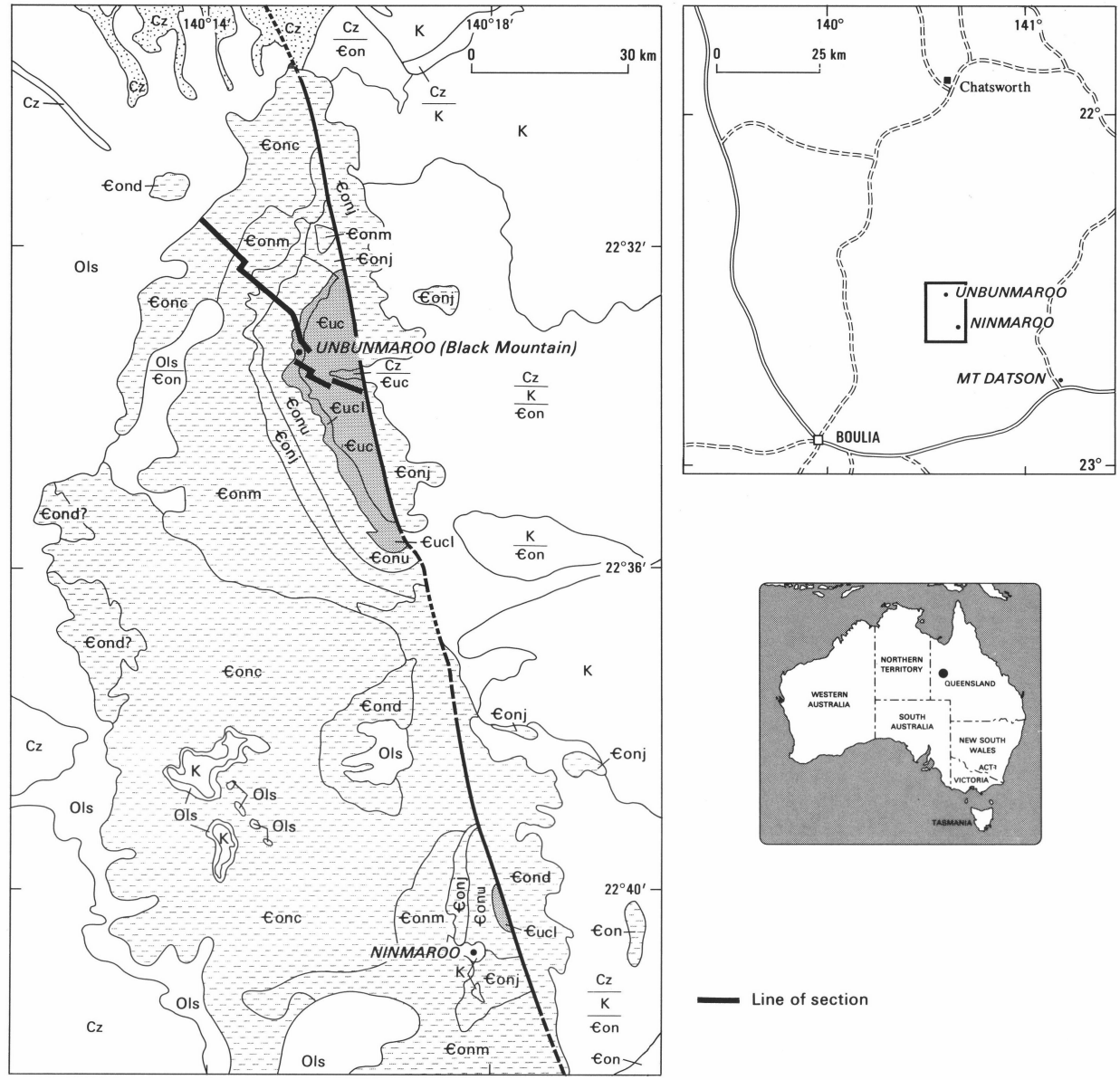

		Cz	*Alluvium, sand, black and brown soil, clay*
CRETACEOUS		K	*Sandstone, ferruginous sandstone, conglomerate, siltstone, claystone*
ORDOVICIAN TO TERTIARY	Digby Peaks Breccia	OTb	*Silcrete, silicified ferruginized chert, breccia*
	Swift Formation	Ols	*Sandstone, siltstone, coquinite (all silicified in part), chert*
EARLY ORDOVICIAN	NINMAROO FORMATION	€on	*Limestone*
	Datson Member	€ond	*Thin bedded limestone or dolomite with interbedded chert*
	Corrie Member	€onc	*Limestone (pelmatozoan, peloid, clast and ooid grainstone) dolomitic sandstone, calcareous siltstone*
	Mort Member	€onm	*Limestone (intraclast, ooid and peloid grainstone calcareous siltstone)*
	Jiggamore Member	€onj	*Thin to thick bedded limestone (peloid and intraclast grainstone, micrite, two-toned limestone), calcareous siltstone*
	Unbunmaroo Member	€onu	*Medium to thick bedded limestone (intraclast and peloid grainstone, mudstone, stromatolitic boundstone), dolomite, calcareous siltstone*
LATE CAMBRIAN	CHATSWORTH LST — Lily Creek Member	€ucl	*Calcareous cross stratified sandstone, sandy limestone, calcareous siltstone*
		€uc	*Thin bedded light to medium grey limestone (peloid grainstone), limestone, calcareous siltstone*

20/F54-10/1

Figure 1. Locality map, showing geology of the Black Mountain (Unbunmaroo) and Ninmaroo inliers.
The location of the section line is indicated.

and erect cusps on P elements: *C. prolindstromi* — *C. lindstromi* — *C.* sp. nov. B and *C. prion*. The second consists of species with laterally compressed S elements and P elements in which the anterior margin of the basal cavity curves around in a groove to meet the antero-basal corner: *C. angulatus* Pander (1856) and *C. horridus* Barnes & Poplawski (1973). The third lineage consists of the robust forms with P elements that have rounded anterior margins and cusps that are round in section and strongly recurved: *C. pararotundatus* Olgun (1987), *C. caseyi* Druce & Jones (1971) and *Cordylodus ramosus* Hadding (1913).

Four species of the biapical lineage (Fig. 2) are distinguished in this study. Two species, *C. prion* Lindström, 1955, and *C. lindstromi* Druce & Jones, 1971 have been previously recognised. One species, *C. prolindstromi* sp. nov., is named in this paper and a fourth species, *C.* sp. nov. B, remains in open nomenclature. These four species are regarded as representing a distinct branch of the genus *Cordylodus,* but are not considered to be significantly distinct to warrant establishment of a new genus to contain this evolutionary lineage. The presence of multiple apices in basal cavities of early forms such as *C. proavus* (Andres, 1988) supports this approach.

Stratigraphic distribution and morphological similarity indicate that *Cordylodus prolindstromi,* the earliest member of the biapical lineage, probably evolved from *C. caboti*. The two species are distinguished by the shape of the P elements and by the biapical basal cavity in *C. prolindstromi*.

Significance of the biapical basal cavity

The presence of a biapical basal cavity in conodonts is not restricted to some species of *Cordylodus,* but is also found in genera such as *Icriodus, Iapetognathus* and *Pelekysgnathus*. In *Cordylodus* the anterior, or primary, cavity apex extends into the cusp, and the secondary cavity apex extends into the first denticle of the posterior process. Andres (1988) has illustrated specimens of *C. proavus* with up to five secondary cavity apices extending into denticles along the entire the posterior process, but the species detailed here have only two apices.

The biapical basal cavity is best developed in the S elements and is sometimes observable in some P elements. The M element usually lacks a second cavity apex, except in *C. prion*.

The function of the secondary cavity apex is not apparent. In the material examined, the secondary cavity extends only a short distance toward the oral surface of the element and does not reach the white matter in the denticle. The pointed apex of the basal cavity of conodonts is a reduction of the cavity that in primitive conodonts extended up the hollow cone to the cusp apex. There seems to be no physiological or structural advantage in developing a hollow cone in a second denticle or cusp. The depth of the secondary apex is not great enough to strengthen the adhesion of the cusp to the basal cavity.

The secondary basal cavity apex does not appear to have biological advantage for the animal, but it is a useful morphological character in the recognition of a group of *Cordylodus* species.

Biostratigraphic implications

In the Black Mountain type section of the Ninmaroo Formation (Radke, 1981), the ranges of *C. caboti, C. prolindstromi, C. lindstromi* and *C.* sp. nov B have been documented in the recent sample set (Fig. 3). The highest appearance of *C. caboti* is 316 m, above the base of the formation (sample BMA 115). *C. prolindstromi* first appears at 329 m (sample GB90-002/3) and continues through to 390 m (sample GB90-002/38). *C. lindstromi* first appears at 404 m (sample GB90-002/51) and continues through to 572 m (sample GB90-002/109). *C.* sp. nov. B occurs only at 495.8 m (sample GB-002/96). *C. prion* has not been found in the Ninmaroo Formation, or at any other locality in Australia.

Nicoll (1990, table 3) has noted the presence of biapical *Cordylodus* elements with flattened second apex in samples of the Ninmaroo Formation collected by Druce & Jones (1971). Such elements occur in both the Mt Datson and Mt Ninmaroo sections, below the first appearance of 'normal' elements of *C. lindstromi*. These elements are now interpreted as elements of *C. prolindstromi* and their stratigraphic distribution agrees with that observed in the Black Mountain section.

The identification of *C. prolindstromi* as a precursor species at a stratigraphic level just below the first occurrence of *C. lindstromi* should allow the first appearance datum (FAD) for *C. lindstromi* to be used as an accurate time line for correlation. If other sections with the same faunal succession can be located, the *C. prolindstromi–C. lindstromi* boundary could have great biostratigraphic significance.

The relationship of *C. prion* to other biapical *Cordylodus* species is difficult to determine until more is known about its stratigraphic range. This will require re-examination of material from other sections, such as Green Point, Newfoundland, where Barnes (1988, fig. 13k,l) illustrates a specimen that conforms to the definition of *C. prion* used here. Barnes (1988) recovered the specimen from Green Point sample 52, which is very low in the reported range of *C. lindstromi* and just above the last occurrence of *Hirsutodontus simplex*. *C. prion* may have evolved directly from *C. prolindstromi,* and would thus be essentially time equivalent with *C. lindstromi*.

The type of *C. prion,* at Stora Backor sample 5 (Lindström, 1955) (where this species co-occurs with *C. angulatus)* occurs in a conodont fauna that has many reworked elements from a variety of Late Cambrian or Early Ordovician ages. Some species of *Cordylodus* in the Stora Backor sample may be reworked, and thus provide no stratigraphic information about the range of the genus or its species.

Conclusions

This study has distinguished four species of *Cordylodus,* all with biapical basal cavities. Three of these species have been recovered from samples of the Ninmaroo Formation in the Georgina Basin of Australia. Two species, *C. prolindstromi* and *C. lindstromi,* are distinguished by the degree of development of the secondary apex of the basal cavity, as well as other morphological characteristics. In the Ninmaroo Formation, *C. prolindstromi* occurs stratigraphically below *C. lindstromi*. *C. lindstromi* probably therefore evolved from *C. prolindstromi* with the modification of the second basal cavity apex from flat to pointed.

Evidence of the possible evolution of *C. lindstromi* from *C. prolindstromi* makes the FAD of the former a closely controlled datum that might be the appropriate level for the Cambrian–Ordovician boundary. However, this relationship would have to be documented in other sections to be acceptable.

The third species, *C.* sp. nov B, appears to have evolved from *C. lindstromi* as the elements become very laterally compressed.

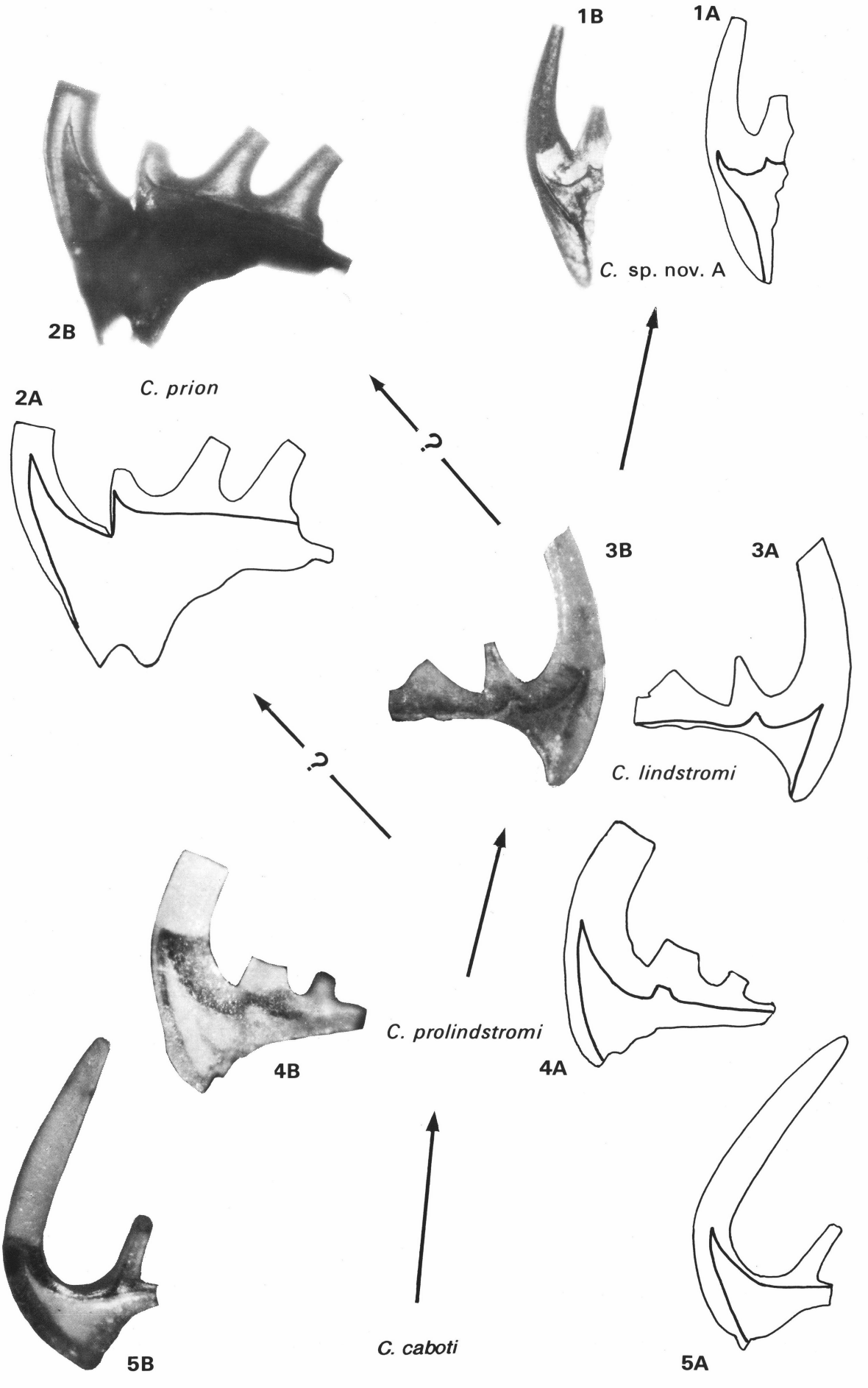
1B
1A
C. sp. nov. A
2B
C. prion
2A
?
3B
3A
?
C. lindstromi
C. prolindstromi
4B
4A
C. caboti
5B
5A

The relationship of *C. prion* to *C. lindstromi* will have to be determined in sections in Europe and North America, rather than in Australia, where the former species has not been recorded.

Taxonomy

Cordylodus Pander, 1856

Type species. *Cordylodus angulatus* Pander, 1856

Diagnosis (emended). Septimembrate apparatus of ramiform elements. The element types M, Sa, Sc, Sb, Sd, Pb and Pa are distinguished. The upper portion of the cusp is composed of white matter. The S and P elements have a denticulate posterior process, and the M element a lateral process, which may or may not be denticulate. Extent of penetration of the basal cavity into cusp highly variable and species-dependent. Some species may have two apices to the basal cavity (biapical), with the primary apex extending into the cusp and the secondary apex into first denticle of the posterior process. Occasional elements may have more than two basal cavity apices, with apices extending into several denticles along the posterior process (Andres, 1988). Short adentate lateral processes may be found on some elements of some species. Element surface smooth, lacking micro-ornamentation, but some elements have carina or keels.

Remarks. Nicoll (1990) has recently examined the apparatus structure of the genus *Cordylodus* and the fauna examined in this study appears to confirm his observations.

Cordylodus caboti Bagnoli, Barnes & Stevens, 1987
Fig. 2.5

Synonymy

v. 1971 *Cordylodus oklahomensis* Müller; Druce & Jones, p. 69, pl. 5, figs 6,7, text-fig. 23j

1987 *Cordylodus caboti* n. sp.; Bagnoli, Barnes & Stevens, p. 152, pl. 1, figs 10–14

1987 *Cordylodus intermedius* Furnish; Bagnoli, Barnes & Stevens, pp. 153–154, pl. 1, figs 15–18

v. 1990 *Cordylodus* sp. nov. A; Nicoll, pp. 552–554, fig. 23

Remarks. Nicoll (1990) indicated that his *Cordylodus* sp. nov. A might be assigned to *C. caboti;* additional material now confirms that assignment. Bagnoli & others (1987) believed that they could separate *C. caboti* and *C. intermedius*. Material examined from the Ninmaroo Formation indicates that these species should be considered as conspecific. Nicoll (1990) indicated that the type of *C. intermedius* Furnish (1938) is conspecific with *C. angulatus*. Much of the *Cordylodus* material from the *Hirsutodontus simplex* Zone that has previously been assigned to *C. intermedius* should therefore probably be assigned to *C. caboti*. The basal cavity of *C. caboti* has a single basal cavity apex.

Distribution. At Black Mountain: Jiggamore Member, Ninmaroo Formation, below 316 m (highest recovery sample BMA 115).

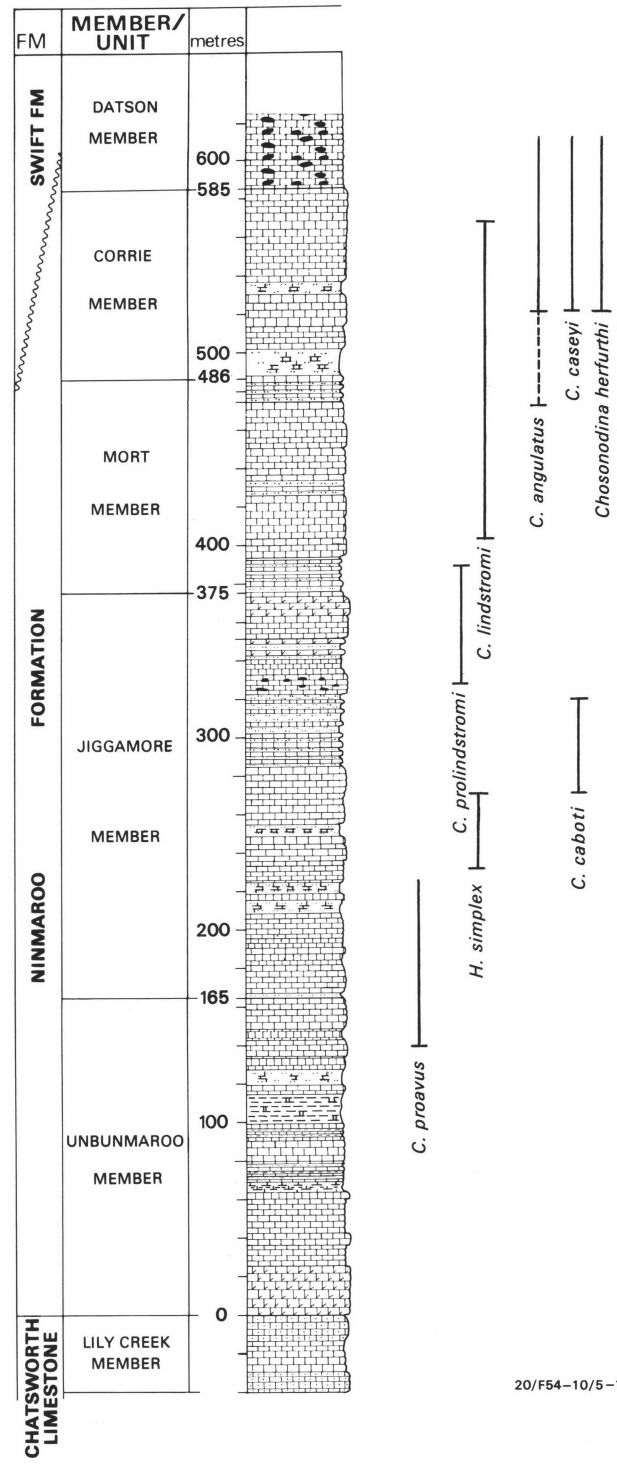

Figure 3. Stratigraphic distribution of selected conodont species in the Ninmaroo Formation section, Black Mountain, Georgina Basin, Queensland.

Figure 2 (facing page). Evolution of the basal cavity shape in S elements of *Cordylodus*.
The sequence from *C. caboti* to *C.* sp. nov. B is documented in the Ninmaroo Formation at Black Mountain (Figure 3). *C. prion* has not been found in Australia and its precise relationship in the evolutionary sequence is not known. The A view sketches highlight the basal cavity outline and white matter distribution from the optical photographs of the B views. All figures are lateral views, × 115.
1. *C.* sp. nov. B, Sc element (CPC 23132)[GB90-OO2/96] right element. **2. *C. prion*** Sd element (CPC23082)[JR8-26-82E] left element. **3. *C. lindstromi*** Sc element (CPC 23074)[GB90-002/89] left element. **4. *C. prolindstromi*** Sb element (CPC 23118)[GB90-002/6] right element. **5. *C. caboti*** Sb element (CPC 23072)[BM-JHS-276m] right element.

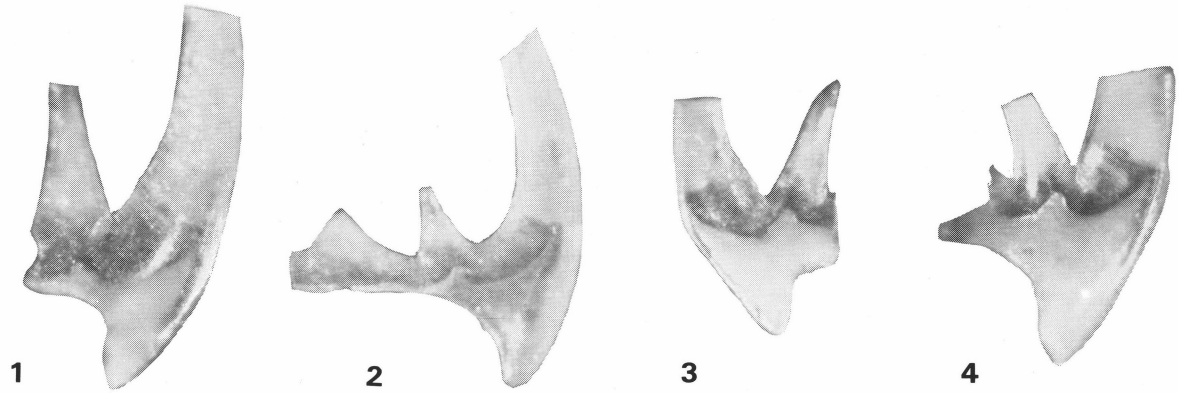

Figure 4. ***Cordylodus lindstromi;*** **lateral views of S elements showing the shape of the basal cavity.**
The posterior process of the Sa, Sb and Sd elements is broken beyond the first denticle. All figures × 125, except as noted.
1. Sa element (CPC 23073)[GB90-002/61] symmetrical element. **2. Sc element** (CPC 23074)[GB90-002/89] left element, inner lateral view, × 110. **3. Sb element** (CPC 23075)[GB90-002/61] left element, outer lateral view, × 115. **4. Sd element** (CPC 23076)[GB90-002/61] right element, outer lateral view.

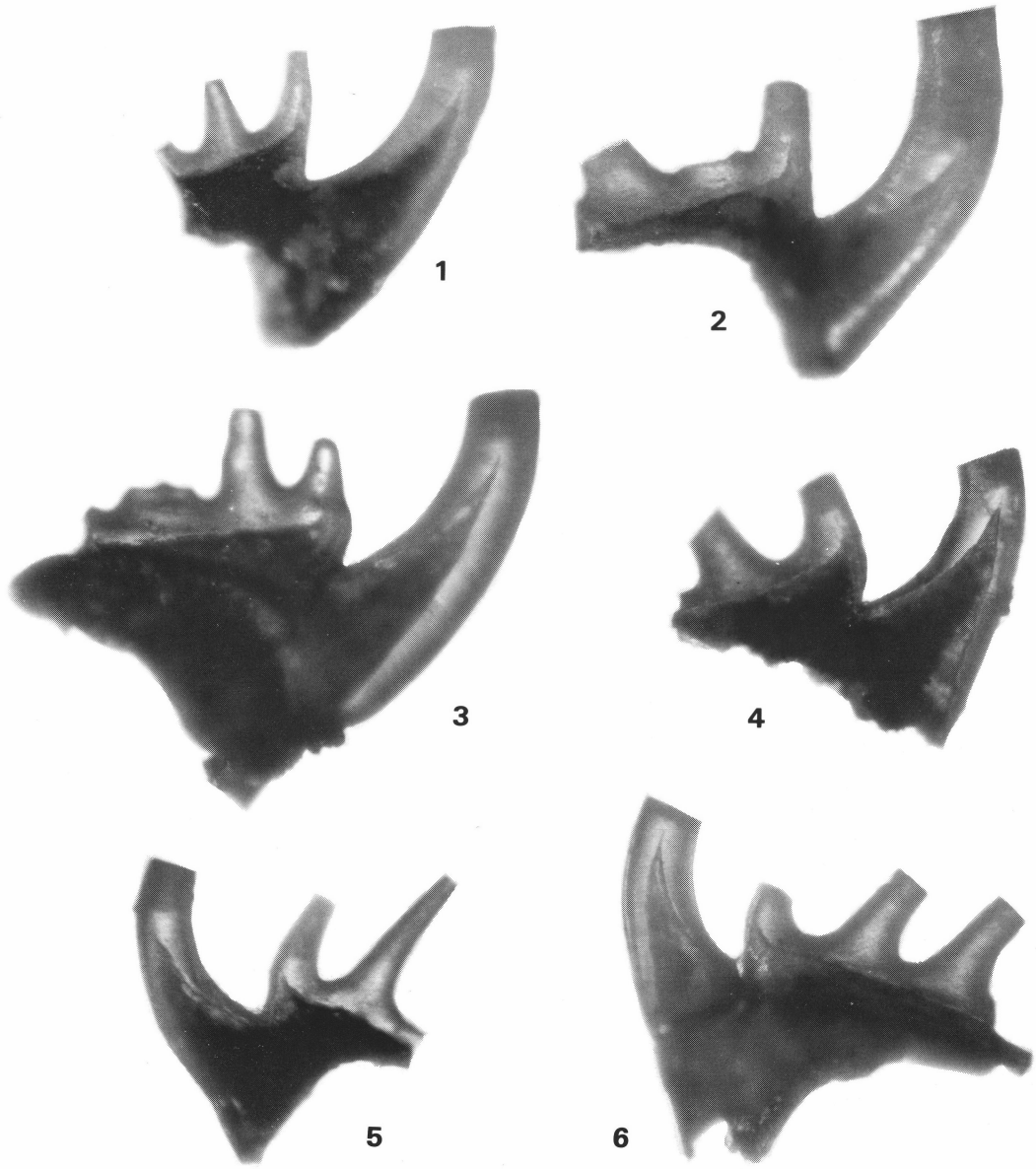

Figure 5. ***Cordylodus prion;*** **lateral views of S elements showing outline shape of dual tipped basal cavity.**
All figures × 120.
1. Sa element (CPC 23077)[JR8-26-82E] symmetrical element. **2. Sa element** (CPC 23078)[JR8-26-82E] symmetrical element. **3. Sb element** (CPC 23079)[JR8-26-82E] right element, outer lateral view. **4. Sc element** (CPC 23080)[JR8-26-82E] left element, inner lateral view. **5. Sd element** (CPC 23081)[JR8-26-82E] left element, outer lateral view. **6. Sd element** (CPC23082)[JR8-26-82E] left element, outer lateral view.

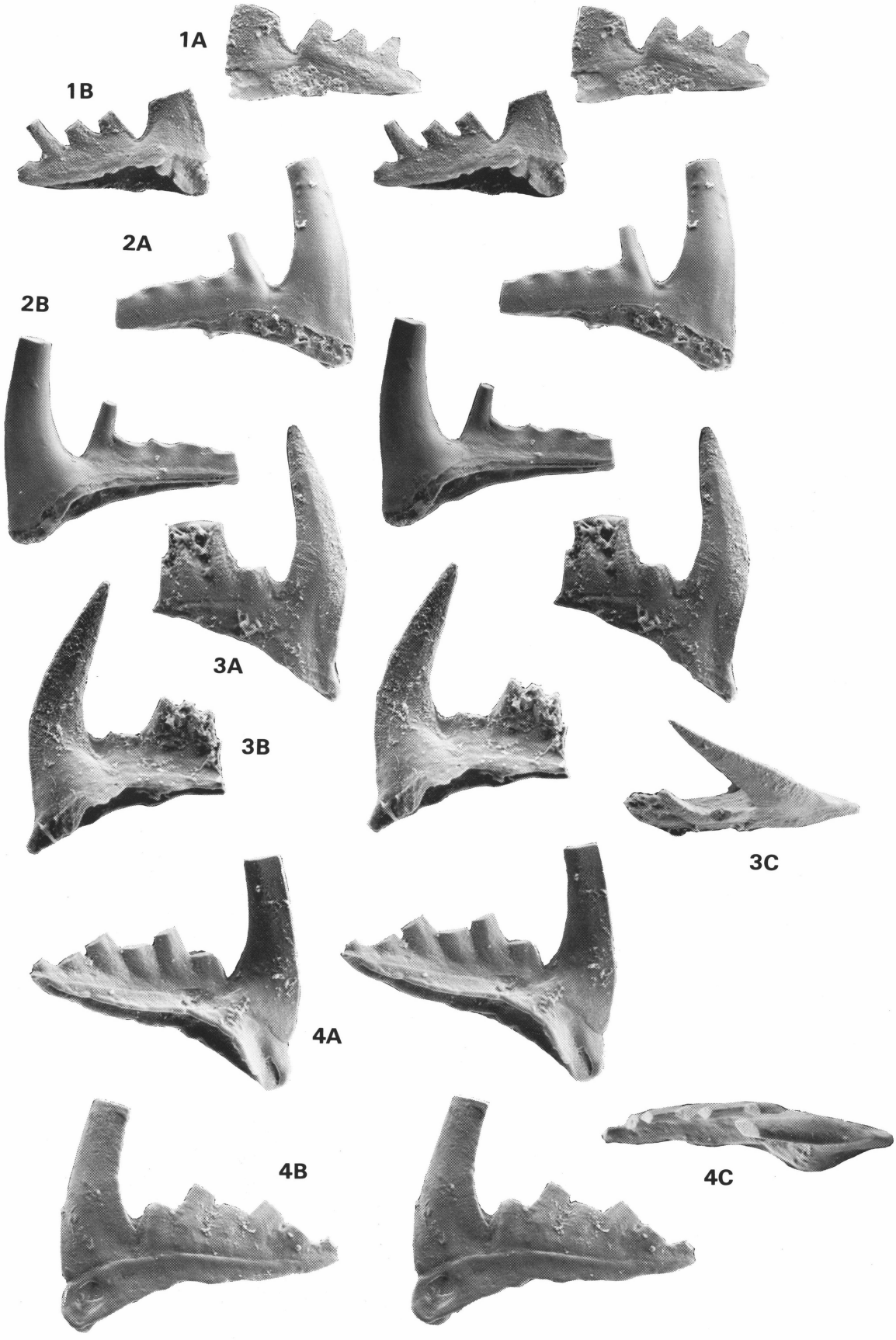

Figure 6. ***Cordylodus prion;*** **M elements.**
All figures × 65.
1. Left element (CPC 23083)[JR8-26-82E]; a, stereo pair, anterior view; **b,** stereo pair, posterior view. **2. Right element** (CPC 23084)[JR8-26-82E]; **a,** stereo pair, anterior view; **b,** stereo pair, posterior view. **3. Right element** (CPC 23085)[JR8-26-82E]; **a,** stereo pair, anterior view; **b,** stereo pair, posterior view; **c,** oral view. **4. Left element** (CPC 23086)[JR8-26-82E]; **a,** stereo pair, posterior view; **b,** stereo pair, anterior view; **c,** oral view.

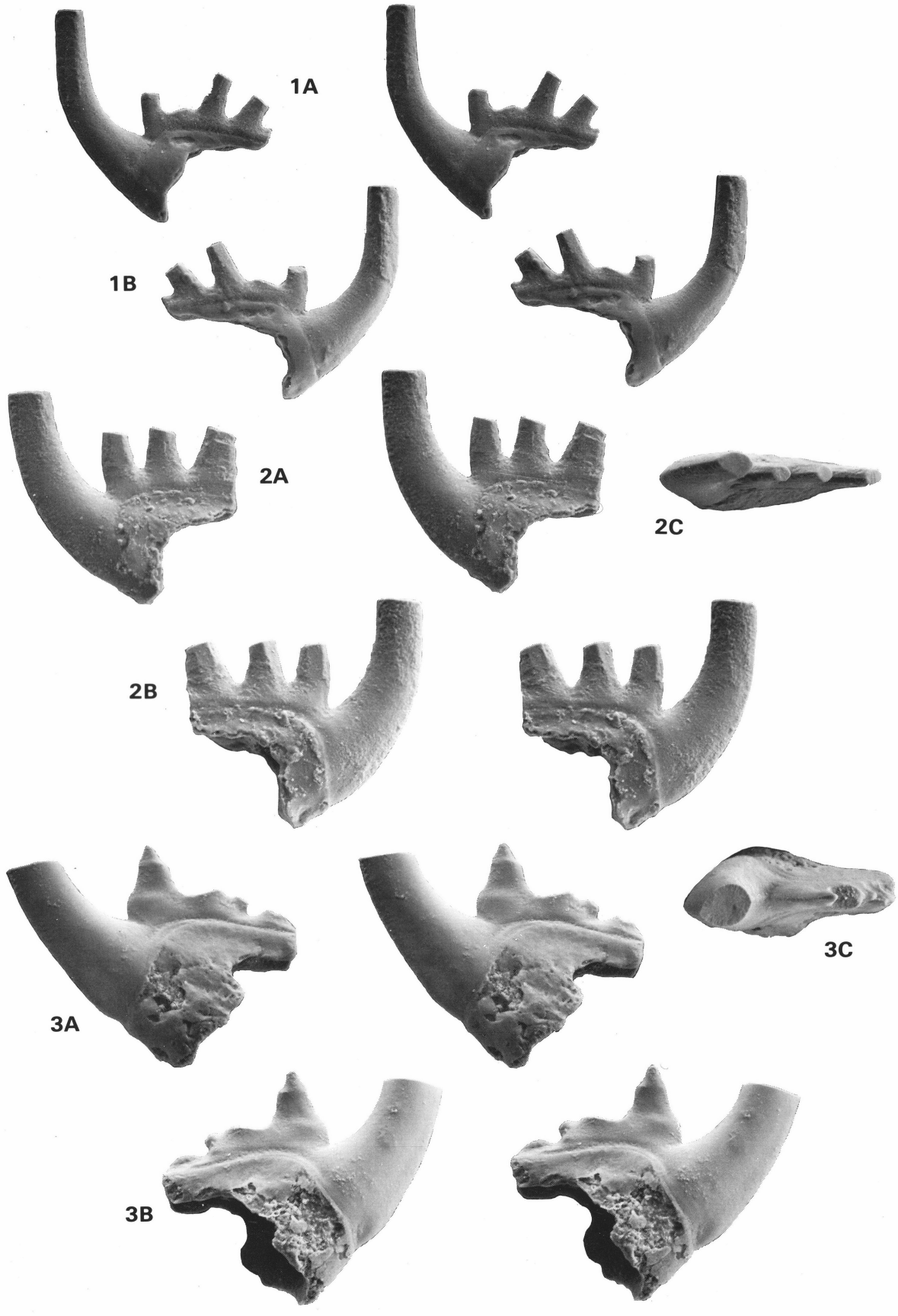

Figure 7. ***Cordylodus prion;*** **Sa elements.**
All figures × 65.
1. (CPC 23087)[JR8-26-82E]; **a,** stereo pair, left lateral view; **b,** stereo pair, right lateral view. **2.** (CPC 23088)[JR8-26-82E]; **a,** stereo pair, left lateral view; **b,** stereo pair, right lateral view; **c,** oral view. **3.** (CPC 23089)[JR8-26-82E]; **a,** stereo pair, left lateral view; **b,** stereo pair, right lateral view, **c,** oral view.

Cordylodus lindstromi Druce & Jones, 1971
Figures 2.3, 2.4

Synonymy.
v. 1971 *Cordylodus lindstromi* n. sp.; Druce & Jones, pp. 68–69, pl. 1, figs 7–9, pl. 2, fig. 8, text-fig. 23h. [Pl. 1, fig. 7 is an Sc element, fig. 8 is an Sc element, fig. 9 is a Pb element and pl. 2, fig. 8 is an Sd element]
v. 1971 *Cordylodus prion* Lindström; Druce & Jones, p. 70, pl. 2, figs 1–7, text-figs. 23i, k-o. [Fig. 1 is a Pa element, figs 2–7 are M elements]
1980 *Cordylodus lindstromi* Druce & Jones; Miller, pp. 18–19, pl. 1, figs 18, 19, text-fig. 4l. [Fig. 18 is an S element and fig. 19 is a Pa element]
1980 *Cordylodus intermedius* Furnish; Miller, pp. 17–18, pl. 1, fig. 17 only. [P element]
1980 *Cordylodus angulatus* Pander; Miller, pp. 13–16, pl. 1, fig. 23 only. [P element]
1981 *Cordylodus caseyi* Druce & Jones; Ethington & Clark, pp. 31–32, pl. 2, fig. 25. [Sd element]
v. 1990 *Cordylodus lindstromi* Druce & Jones; Nicoll, pp. 545–550, figs 3 (2a–c), 16–18.

Material studied. More than 600 elements.

Diagnosis. Septimembrate apparatus of ramiform elements with biapical basal cavity in the S elements and some of the P elements. In most elements the apex of the secondary basal cavity is pointed. The M element is makellate, the Sa element is alate and the remaining elements are dolobrate and asymmetrical. The first denticle of the posterior process is usually very close to the cusp and is frequently touching the posterior cusp margin. Larger elements frequently have a recessive basal margin.

Remarks. Nicoll (1990) re-examined *C. lindstromi* and the material recovered as part of this study does not modify those observations.

Distribution. At Black Mountain: Mort and Corrie Members, Ninmaroo Formation, 404–572 m (samples GB90-002/51 to 109).

Cordylodus prion Lindström, 1955
Figures 2.2, 5–12

Synonymy.
1955 *Cordylodus prion* n. sp. Lindström, pp. 552–553, pl. 5, figs 14–16. [14 M element, 15 Pa element,16 Sc element]
1988 *Cordylodus lindstromi* Druce & Jones; Barnes, p. 410, figs 13j–l, 14 c (only). [13j M element, 13k,l Sa element]
1988 *Cordylodus lindstromi* Druce & Jones; Andres, text-figs 36,37

Material studied. 355 elements (M 22, Sa 42, Sc 116, Sb 88, Sd 44, Pb 30, Pa 13.)

Diagnosis. Septimembrate ramiform apparatus of M, S and P elements. The M element is makellate and denticulate, the Sa element is dolabrate and symmetrical and the Sc, Sb and Sd elements are dolabrate and asymmetrical. The Pb and Pa elements are dolabrate and asymmetrical. The lateral (M element) and posterior processes (S and P elements) are separated from the cusp by a notch and the secondary basal cavity apex is located under the first denticle of the process. All elements have the biapical cavity, but in thicker elements it may be difficult to observe and identification is based on the presence of the notch. The notch and biapical cavity are less prominent in the P elements than in the S elements. The extension of the cavity under the posterior process is offset upward, above the level of the bottom of the notch between the cusp and the first process denticle.

Description. A septimembrate apparatus of *Cordylodus* in which the basal cavity of all elements has a secondary apex extending into the first denticle of the process. In the S elements the posterior process is separated from the cusp by a notch, and the connection of process to cusp is very narrow and weak. If not supported by the basal plate, the posterior process of elements of this species is frequently broken at this point. The extension of the basal cavity from the secondary apex along the underside of the process is higher (Fig. 2.2) than the bottom of the notch separating the process and cusp. This gives the impression of offsetting the posterior process upward. This factor, along with the delectate construction of the process, contributes to the breakage of the process from the cusp.

The Pa and Pb elements (Figs 11, 12) are dolabrate and the basal cavity opens downward with a groove extending posteriorly under the posterior process. In both elements the upper part of the cusp is inside the axial line of the posterior process. Denticles are laterally compressed and usually have sharp keels.

The Pa element is laterally compressed and the cusp is relatively longer, as a proportion of the total element length, than the cusp of the Pb element. The Pa element cusp is reclined; the denticles are also reclined and closely spaced. The keel on the anterior margin of the cusp terminates above the base and the anterobasal corner is rounded.

The Pb element has an erect cusp at the base, but is gently recurved posteriorly above the apex of the basal cavity. As in the Pa element, the anterior margin of the cusp may have a sharp keeled margin extending toward the anterobasal corner, but this keel stops above the base and the anterobasal margin is rounded. The process denticles of the Pb element are not usually as closely spaced as those of the Pa element, and they are usually taller and more erect.

The M element (Fig. 6) is makellate; the outer lateral process supports 6 or more denticles in large elements. The very short anticusp lacks denticles. The anterior margin of the base is essentially straight and the anterior side of the cusp is convex. The cusp is erect, recurved over the buttress, and slightly twisted. The notch between the cusp and the first process denticle is more prominent when viewed from the anterior side, but can also be seen from the posterior side. Process denticles are compressed with sharp keels along the axis of the process. They are appressed at the base but discrete a short distance above the process. Basal plates are well developed on many specimens. The basal cavity opens downward and is broad, extending under the process to the outer lateral tip.

The S elements are all similar, and differ mostly in section view. The posterior process supports 3–5 (occasionally 6 or 7) tall, discrete, laterally compressed denticles that may be fused at the base. The base of the process lacks height, and consists of a series of denticles, fused at their base, resting on the expansive basal plate. The basal cavity opens posteriorly, a feature accentuated by the well-preserved basal plates.

The Sa element is dolobrate and symmetrical; the other S elements are dolobrate and asymmetrical. The posterior process supports up to six discrete laterally compressed ovate denticles. The denticles are erect to recurved. The cusps are similar in lateral view and all extend anteriorly and curve upward.

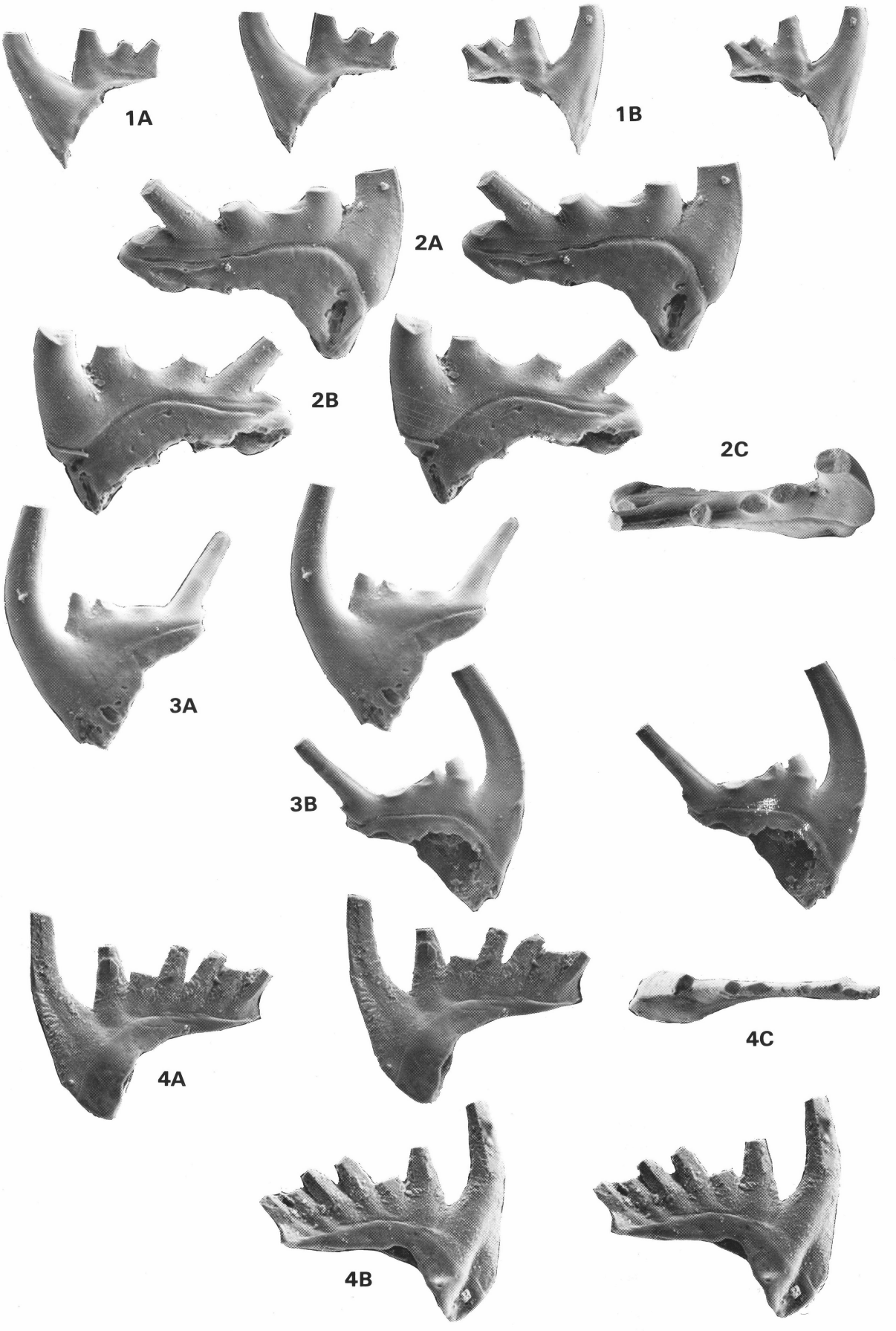
1A
1B
2A
2B
2C
3A
3B
4A
4B
4C

The Sa element (Fig. 7) is symmetrical; the connection of cusp to process is very narrow. The posterior process is straight and supports up to 4 discrete, erect and laterally compressed denticles.

The Sc element (Fig. 8) is asymmetrical; the cusp has a flattened inner cusp face, a convex outer face and a relatively sharp anterior margin. The outer side of the cusp is convex. The cusp is slightly twisted and the upper part may be just outside the axial line of the process. The posterior process is either straight or slightly twisted.

The Sb element (Figs. 9.1, 9.2, 9.4) differs from the Sc element in having a cusp cross-section which is biconvex to rounded. The posterior process is bowed outward.

The Sd element (Figs 9.3, 10) is similar to the Sb element except for a carina on the inner margin of the cusp which extends the inner anterolateral basal margin of the cusp base below the comparable level of the outer anterolateral margin. The anterior face of the Sd element also tends to be flattened. The posterior process appears to be shorter than that of the Sb element.

Remarks. *Cordylodus prion* can be distinguished from *C. lindstromi* by the shape of the basal cavity, the presence of the notch between cusp and process and the greater length of the posterior process. The shapes of the basal cavity of the S elements of *C. caboti, C. prion, C. prolindstromi, C. lindstromi* and *C.* sp. nov. B are shown in Fig. 2. In *C. prion* the extension of the basal cavity under the posterior process is above the level of the low point of the cavity between cusp and first denticle. In *C. lindstromi* and *C. prolindstromi* the basal cavity extension is essentially at the same level as the low point. *C. prion* is the only species of this group to have a secondary cusp tip in the M element.

In *C. prion* the Sa element is dolabrate with a rounded anterior margin. In *C. prolindstromi* the Sa element is also usually rounded, but in some elements the anterior margin is flattened and the element thus appears to be tending toward an alate form. In *C. lindstromi* the Sa element is becoming obviously alate. Thus the dolabrate Sa element of *C. prion* is closer in morphology to *C. prolindstromi* than to *C. lindstromi*. It is possible that *C. prion* evolved directly from *C. prolindstromi*.

In *Cordylodus prion* the connection of the posterior process to the cusp is weak because the upward offset of the basal cavity has reduced the area of the lateral face of the process in contact with the base of the cusp. In *C. lindstromi* and *C. prolindstromi* the process–base cusp join is stronger and the posterior process of these elements is usually intact, or at least not broken between cusp and process.

Reconstruction of the apparatus of *C. prion* from the fauna of the Stora Backor sample was relatively easy All elements of this species have a biapical cavity and it is the only species with a biapical cavity in the fauna. After all the biapical elements were segregated, the similarity of element type morphologies to those of other species of *Cordylodus* made it easier to sort the elements into element types (M, Sa, etc.).

The stratigraphic relationship of *C. prion* and *C. lindstromi* is not well defined because much of the literature has not distinguished the two species. The species are not known to co-occur in Australia or Oklahoma (Miller & others, 1982). Both are found in Newfoundland (Barnes, 1988) low in the range of *C. lindstromi*. The material from Sweden may be reworked, and the association of *C. angulatus* and *C. prion* probably does not indicate true stratigraphic range.

Cordylodus prolindstromi sp. nov.
Figures 2.4, 13–16

Derivation of name. *Pro,* L., before; *lindstromi*, for *Cordylodus lindstromi.*

Material studied. 192 elements (M 52, Sa 18, Sc 49, Sb 31, Sd 31, Pb 6, Pa 5; Table 1)

Diagnosis. Septimembrate apparatus of ramiform elements with an imperfectly developed biapical basal cavity in the S elements and some of the P elements. The M element is makellate, the Sa element dolabrate or alate, and the rest of the elements dolobrate and asymmetrical. The first denticle of the posterior process is usually very close to the cusp and is frequently touching the posterior cusp margin.

Description. The P elements (Fig. 16) are dolabrate, asymmetrical and laterally compressed with rounded anterobasal margin. They have nearly straight posterior processes that have three or four denticles. The cusp of both Pa and Pb elements is straight rather than recurved as in the S elements. In the Pa element the cusp is twisted slightly inward from the plane of the denticles of the posterior process, but in the Pb element the cusp is not inwardly twisted and is in the same plane as the process denticles. The anterior and posterior margins of the cusp are keeled. The basal cavity is shallow, opens downward, and extends posteriorly under the posterior process. The P elements do not have a consistent or well developed secondary basal cavity apex. Some elements (Fig. 16.4) appear to have no hint of a secondary cavity apex. Other elements (Fig. 16.2) have only minor irregularities in the basal cavity in the area under the first process denticle, and some (Fig. 16.1, 16.3) have a distinct irregularity under the denticle, but not a well defined secondary apex.

Table 1. Distribution of *Cordylodus prolindstromi* in the Ninmaroo Formation, Black Mountain, Queensland.
All samples are from section GB90-002, collected in September, 1990, by the author.

Sample	*M*	*Sa*	*Sc*	*Sb*	*Sd*	*Pb*	*Pa*
3	11	4	5	5	7	1	—
4	3	—	2	2	2	—	—
5	2	1	3	2	1	—	—
6	5	5	5	4	6	—	1
7	2	3	3	—	3	—	—
8	10	1	14	2	6	2	2
9	10	—	4	—	2	—	—
10	1	—	—	1	—	—	—
11	1	—	1	3	1	—	—
12	—	—	—	4	1	—	—
13	1	—	1	1	—	—	—
14	—	—	2	2	—	—	—
18	2	1	1	1	—	—	1
19	—	—	1	1	—	—	—
20	2	2	3	4	1	—	1
24	2	1	1	—	—	—	—
38	—	—	3	—	1	3	—
Total	52	18	49	31	31	6	5

Figure 8 (facing page). *Cordylodus prion;* Sc elements.
All figures × 70.
1. Right element (CPC 23090)[JR8-26-82E]; **a,** stereo pair, inner lateral view; **b,** stereo pair, outer lateral view. **2. Left element** (CPC 23091)[JR8-26-82E]; **a,** stereo pair, inner lateral view; **b,** stereo pair, outer lateral view; **c,** oral view. **3. Left element** (CPC 23092)[JR8-26-82E]; **a,** stereo pair, outer lateral view; **b,** stereo pair, inner lateral view. **4. Right element** (CPC 23093)[JR8-26-82E] **a,** stereo pair, inner lateral view; **b,** stereo pair, outer lateral view; **c,** oral view.

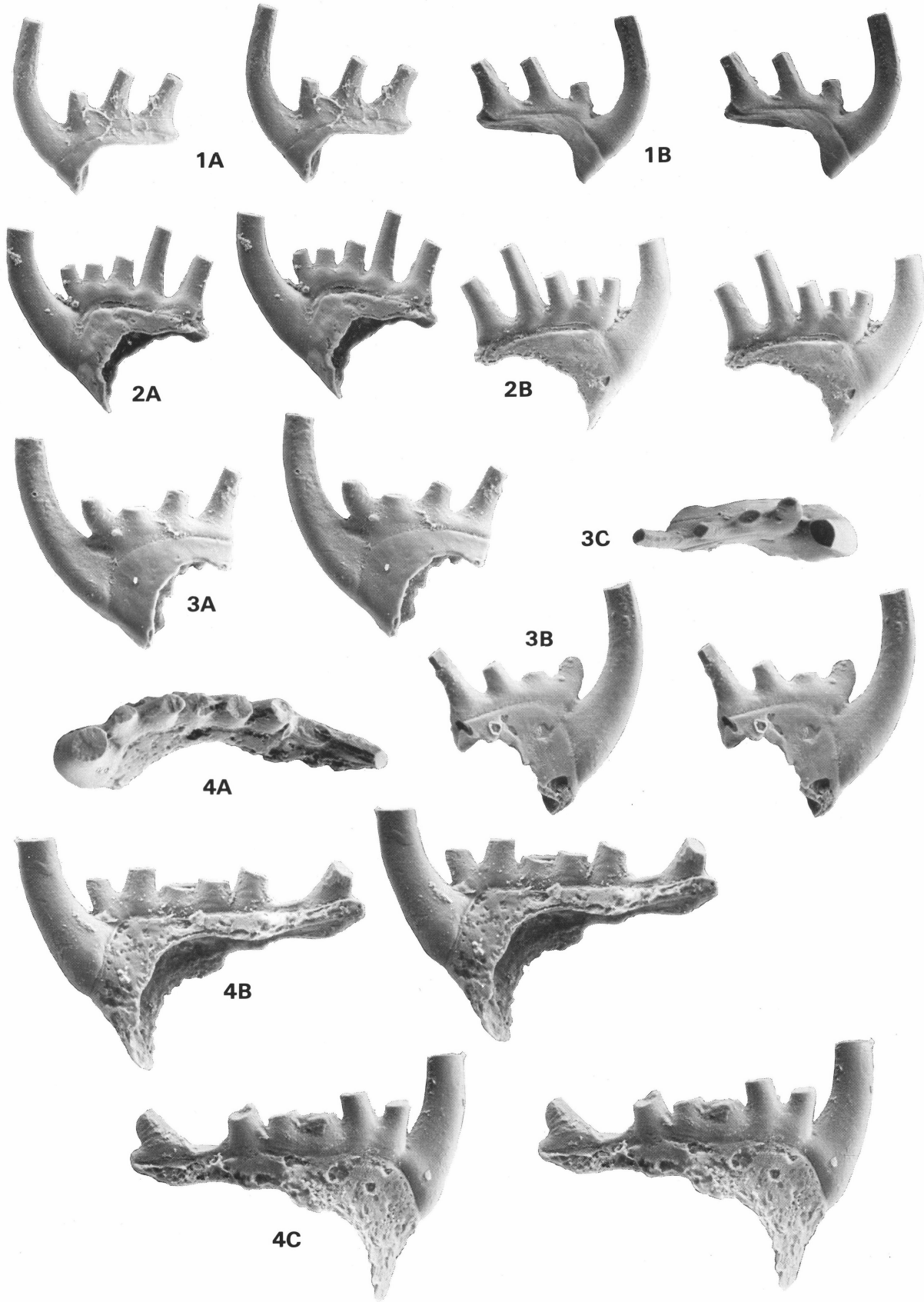

Figure 9. ***Cordylodus prion;*** **Sb and Sd elements.**
All figures × 70.
1. Sb element (CPC 23094)[JR8-26-82E] left element; **a,** stereo pair, outer lateral view; **b,** stereo pair, inner lateral view. **2. Sb element** (CPC 23095)[JR8-26-82E] right element; **a,** stereo pair, inner lateral view; **b,** stereo pair, outer lateral view. **3. Sd element** (CPC 23096)[JR8-26-82E] left element; **a,** stereo pair, outer lateral view; **b,** stereo pair, inner lateral view; **c,** oral view. **4. Sb element** (CPC 23097)[JR8-26-82E] right element; **a,** oral view; **b,** stereo pair, inner lateral view; **c,** stereo pair, outer lateral view.

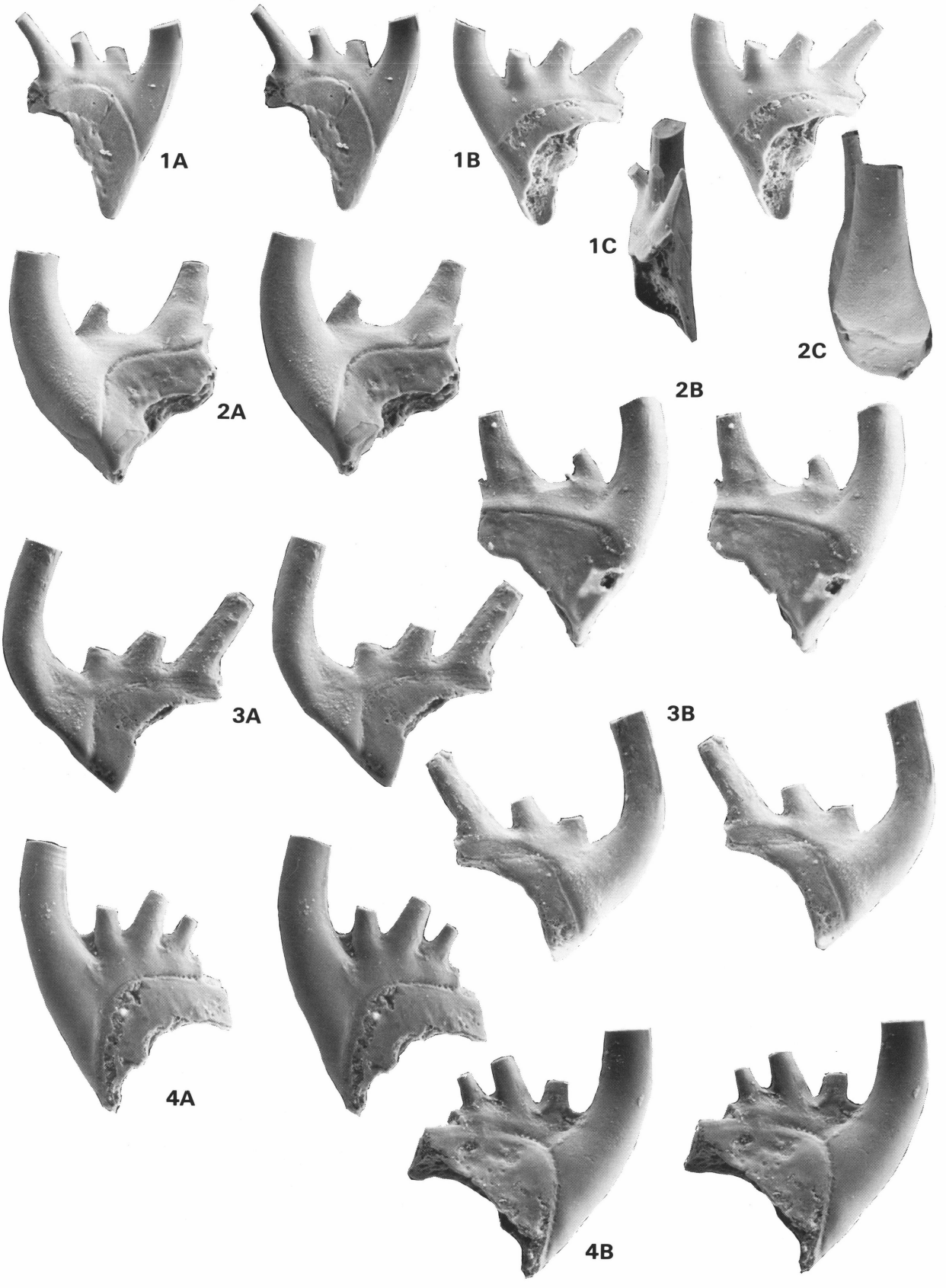

Figure 10. ***Cordylodus prion;*** **Sd elements.**
All figures × 70.
1. Left element (CPC 23098)[JR8-26-82E]; **a,** stereo pair, inner lateral view; **b,** stereo pair, outer lateral view; **c,** posterior view. **2. Right element** (CPC 23099)[JR8-26-82E] **a,** stereo pair, outer lateral view; **b,** stereo pair, inner lateral view; **c,** anterior view. **3. Right element** (CPC 23100)[JR8-26-82E]; **a,** stereo pair, inner lateral view; **b,** stereo pair, outer lateral view. **4. Left element** (CPC 23101)[JR8-26-82E]; **a,** stereo pair, outer lateral view; **b,** stereo pair, inner lateral view.

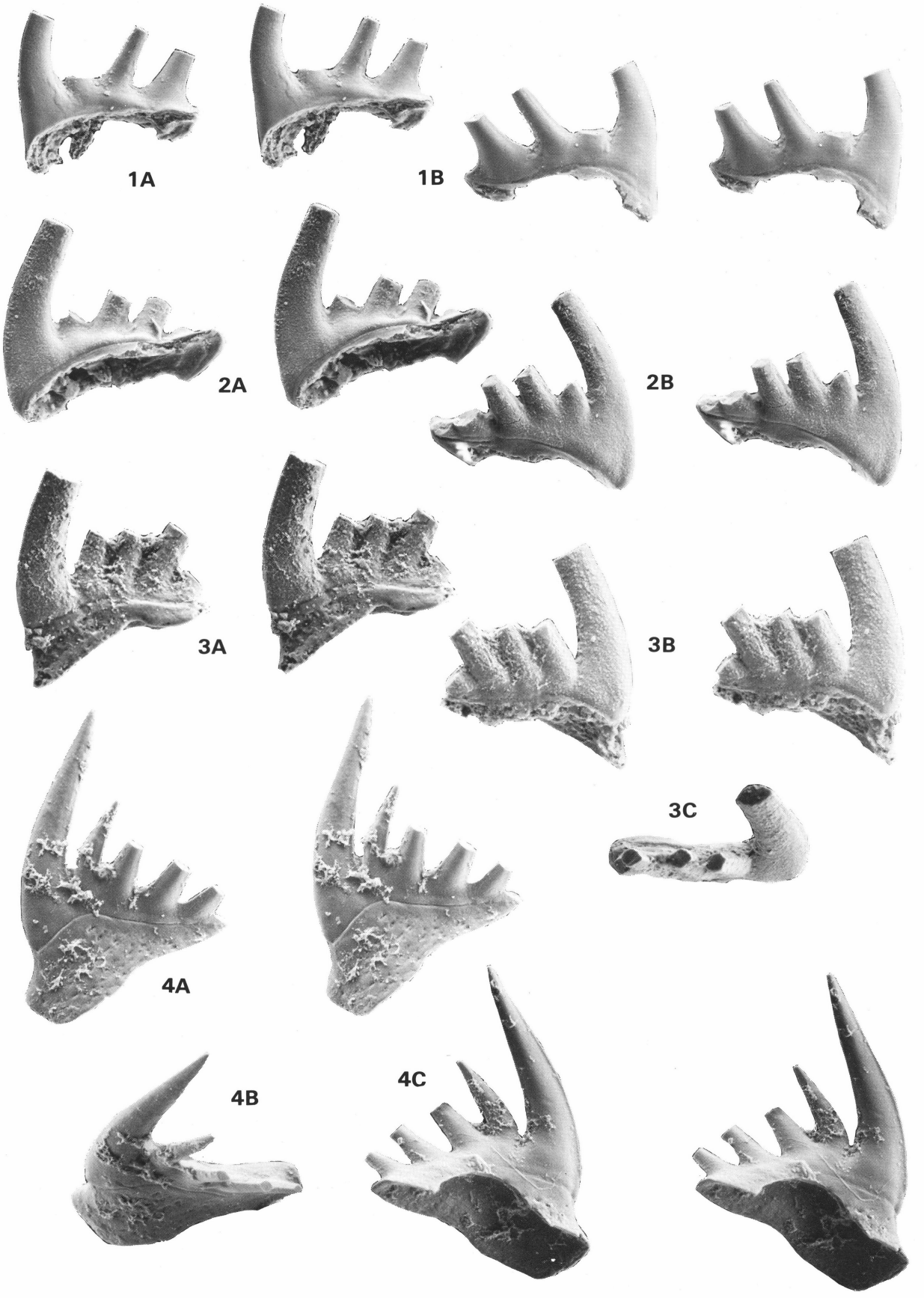

Figure 11. ***Cordylodus prion;*** **Pb elements.**
All figures × 70.
1. Right element (CPC 23102)[JR8-26-82E] ; **a,** stereo pair, inner lateral view; **b,** stereo pair, outer lateral view. **2. Right element** (CPC 23103)[JR8-26-82E] **a,** stereo pair, inner lateral view; **b,** stereo pair, outer lateral view. **3. Right element** (CPC 23104)[JR8-26-82E]; **a,** stereo pair, inner lateral view; **b,** stereo pair, outer lateral view; **c,** oral view. **4. Left element** (CPC 23105)[JR8-26-82E]; **a,** stereo pair, outer lateral view; **b,** oral view; **c,** stereo pair, inner lateral view.

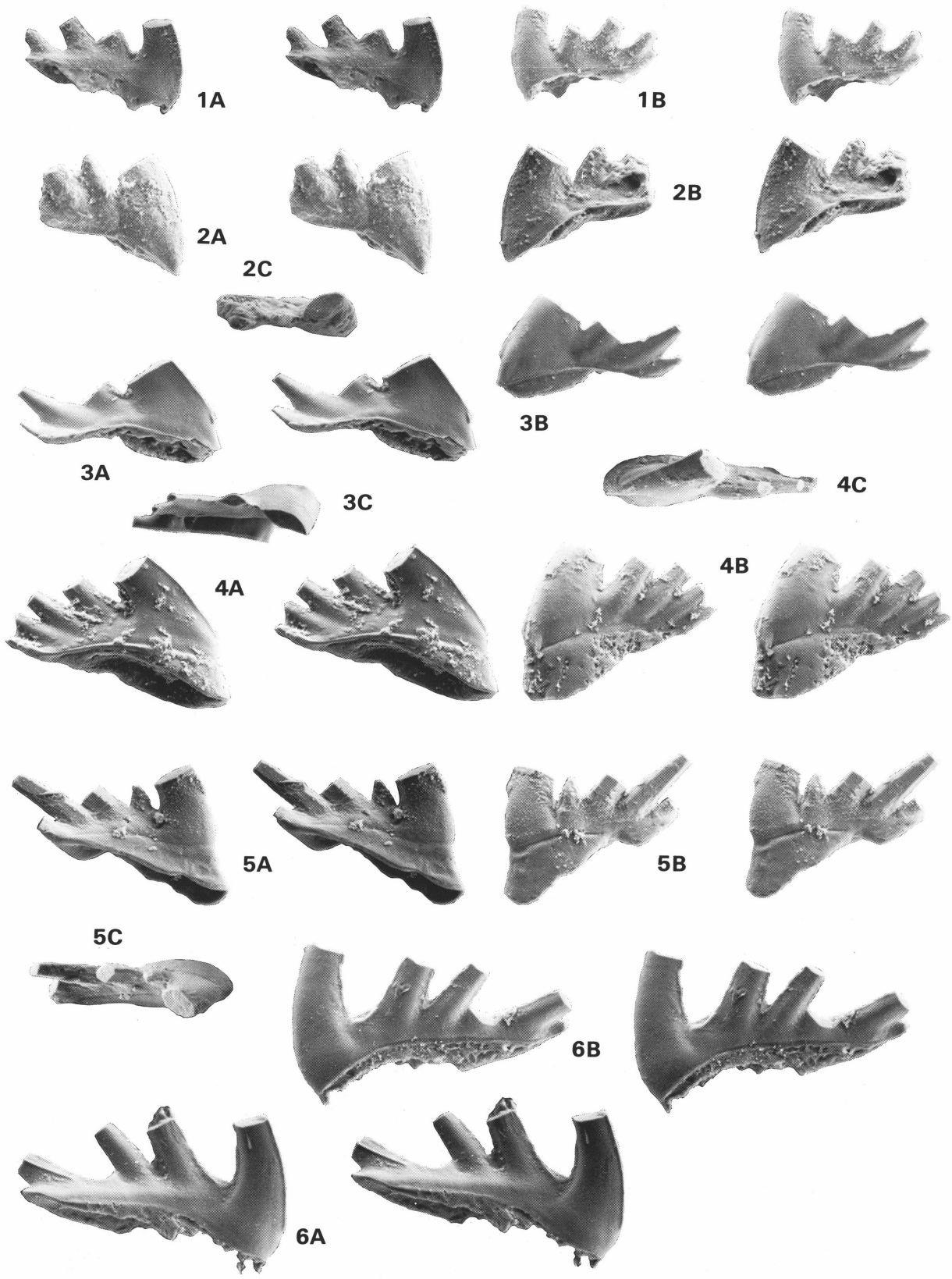

Figure 12. ***Cordylodus prion;*** **Pa and Pb elements.**

All figures × 70.

1. Pb element (CPC 23106)[JR8-26-82E] left element; **a,** stereo pair, inner lateral view; **b,** stereo pair, outer lateral view. **2. Pa element** (CPC 23107)[JR8-26-82E] right element; **a,** stereo pair, outer lateral view; **b,** stereo pair, inner lateral view; **c,** oral view. **3. Pa element** (CPC 23108) left element; **a,** stereo pair, inner lateral view; **b,** stereo pair, outer lateral view; **c,** oral view. **4. Pa element** (CPC 23109)[JR8-26-82E] left element; **a,** stereo pair, inner lateral view; **b,** stereo pair, outer lateral view; **c,** oral view. **5. Pb element** (CPC 23110) left element; **a,** inner lateral view; **b,** stereo pair, outer lateral view, **c,** oral view. **6. Pb element** (CPC 23111)[JR8-26-82E] left element; **a,** stereo pair, inner lateral view; **b,** stereo pair, outer lateral view.

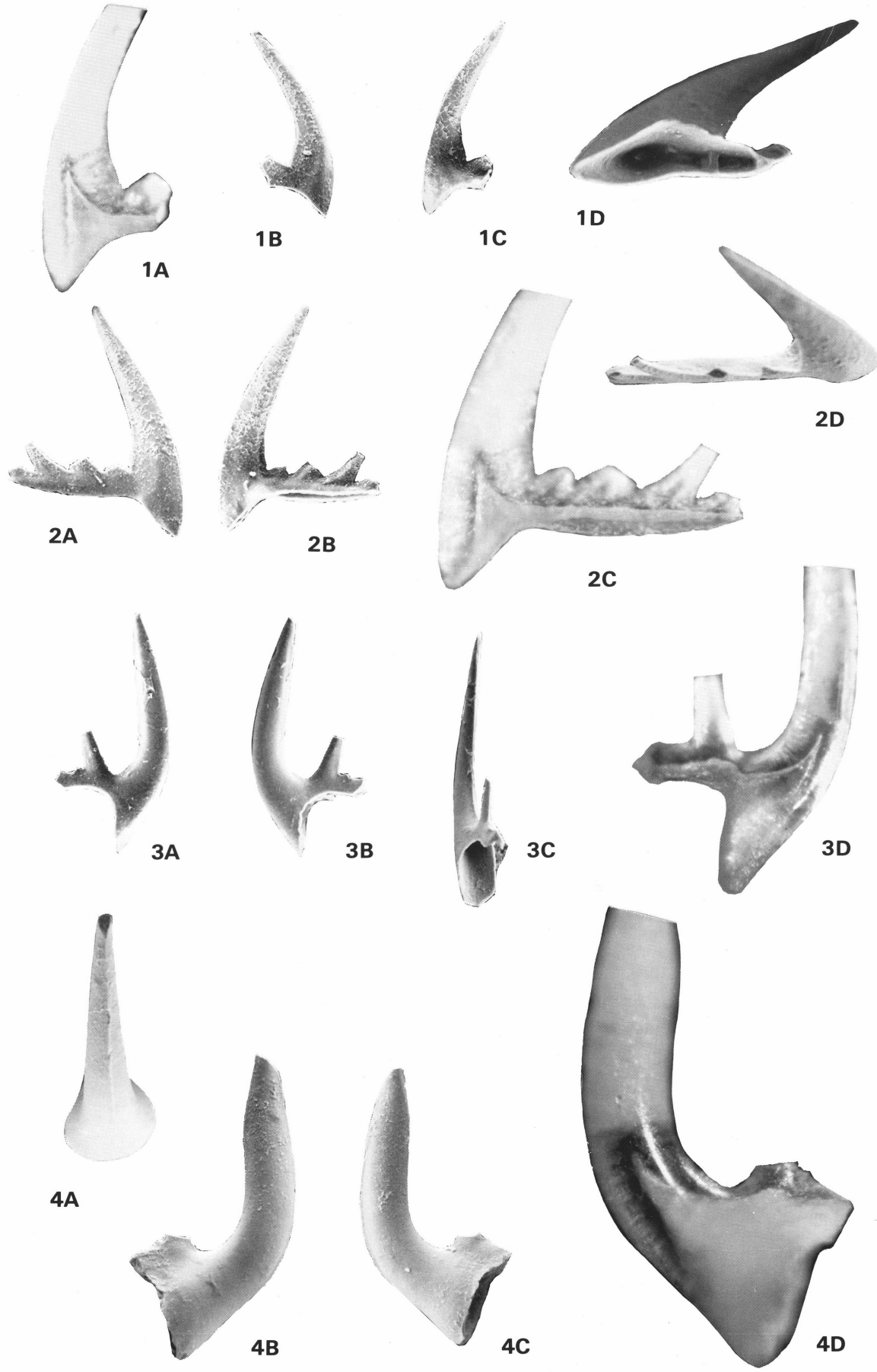
1A
1B
1C
1D
2A
2B
2C
2D
3A
3B
3C
3D
4A
4B
4C
4D

The M element (Fig. 13) is makellate and has an erect, antero-posteriorly compressed cusp with a buttress on the posterior face, and a denticulate outer-lateral process. The process supports four to six triangular denticles that are appressed at the base. The cusp is slightly recurved posteriorly over the buttress. The M element has only a single basal cavity apex.

The S elements have erect to recurved cusps composed of white matter extending down to the apex of the basal cavity. The apex of the primary basal cavity is central in some elements and close to the anterior margin in others. The secondary basal cavity is located under the first denticle of the posterior process; its shape and degree of development are variable. The basal cavity opens posteriorly and downward with a groove extending under the posterior process. The cusp is laterally compressed with a sharp margin or keel on both anterior and posterior margins where the cusp is composed of white matter. Process denticles are laterally compressed with sharp margins.

The Sa element (Fig. 13) is dolabrate, becoming alate in some elements, and bilaterally symmetrical with a short denticulate posterior process and laterally compressed cusp that has keels on both the anterior and posterior margins. The keel of the anterior margin disappears toward the base and the anterobasal margin is rounded.

The Sc element (Fig. 14) is dolabrate and asymmetrical with the inner side flattened and the outer side convex. The inner anterior edge is only slightly thickened and the anterior margin is sharp. The Sb element (Fig. 14) is dolabrate and similar to the Sc element except that it is biconvex with a rounded lower anterior margin.

The Sd element (Fig. 15) is dolabrate and asymmetrical with a convex outer side and a slightly concave inner side. The inner lateral rim near the anterior margin is sharp in juvenile forms, but becomes rounded and more prominent in older specimens. The posterior process is bent slightly inward after the first process denticle.

Remarks. *Cordylodus prolindstromi* can be distinguished from *C. lindstromi* by a number of morphological characters. In *C. prolindstromi* the second apex of the basal cavity is usually truncated, frequently with a flat top, while in *C. lindstromi* the second cavity apex is usually pointed. In *C. prolindstromi* the anterior margin of the Sa element is rounded, but in *C. lindstromi* it is flattened, especially toward the base. The Sd element of *C. lindstromi* has the posterior process bent strongly inward, but in *C. prolindstromi* the posterior process is only slightly bent. In the material examined, no elements of *C. prolindstromi* have recessive basal margins, a feature observed in some larger elements of *C. lindstromi*.

Distribution. At Black Mountain: Jiggamore and lower part Mort Members, Ninmaroo Formation, 331–385 m (samples GB90-002/3 to 43).

Cordylodus sp. nov. B
Figures 2.1, 17–18

Material studied. 8 elements (M 2, Sa 1, Sc 2, Sb? 2, P 1)

Diagnosis. Multimembrate ramiform apparatus of gracile, laterally compressed elements. Probable septimembrate apparatus with 5 element types (M, Sa, Sc, Sb or Sd, and P) recognised in this study. The S elements have a biapical basal cavity.

Description. The single P element recovered (Fig. 18.3) is dolabrate, asymmetrical and laterally compressed, and is dominated by a tall triangular cusp with a low carina on the inner face that extends toward the basal margin. The anterior and posterior margins are sharp with a posterior process that is broken, but which has two preserved denticles. The basal outline is biconvex; the basal cavity has a single apex extending into the cusp and a shallow channel extending posteriorly under the process. The element illustrated is probably a Pb element because the cusp and process denticles are in the same plane, but without more material Pa and Pb elements cannot be safely differentiated.

The M element (Fig 17.1, 2) is makellate, anteriorly-posteriorly compressed with a flat anterior face and a very small buttress on the posterior face. The outer lateral process supports at least two denticles that are laterally appressed at the base with sharp margins. The basal cavity has a single apex extending into the cusp to the base of the white matter, about one quarter to one third of the height of the cusp.

The S elements, like the M and P elements, are compressed. They have a low, but prominent, secondary cavity apex. The primary basal cavity apex terminates near the anterior margin of the element. The Sa element (Fig. 17.3) is dolabrate, trending toward being alate, symmetrical, and has a flattened anterior margin with sharp lateral edges. There is at least one denticle on the posterior process.

The Sc element (Fig. 17.4,5) is dolabrate and asymmetrical. The outer face is convex with a rounded outer lateral margin. The inner face is flat and the inner antero-lateral margin is sharp. The antero-basal area is large and points downward, almost like the anticusp of an M element. There is at least one laterally compressed denticle on the posterior process.

The remaining element (Fig. 18.2,3) is probably an Sb element, or, less likely, an Sd element. The anterior margin appears rounded, a characteristic feature of the Sb element. The element is dolabrate, biconvex and asymmetrical in cross-section with the anterior margin bent inward.

Remarks. Too few elements of *Cordylodus* sp. nov. B have been recovered to describe this species accurately or fully. The eight elements from sample GB90-002/96 can be assigned to five element types. However, all of the elements are markedly laterally compressed, much more so than the S elements of *C. angulatus*. The S elements also have a biapical basal cavity. On these two characters alone, elements assigned to *C.* sp. nov. B should be easily differentiated from other species of *Cordylodus*. The large triangular (in lateral view) cusp of the P element could have been derived from an elongation of the cusp of *C. lindstromi*.

Distribution. At Black Mountain: lower part of the Corrie Member, Ninmaroo Formation, 495.8 m (sample GB90-002/96).

Figure 13 (facing page). ***Cordylodus prolindstromi;*** **M and Sa elements.**
All figures × 70, except as noted.
1. M element (paratype CPC 23112)[GB90-002/9] right element; **a,** posterior view to show basal cavity outline (× 120); **b,** anterior view; **c,** posterior view; **d,** basal view (× 170). **2. M element** (paratype CPC 23113)[GB90-002/9] right element; **a,** anterior view; **b,** posterior view; **c,** posterior view showing outline of the basal cavity (× 120); **d,** oral view (× 110). **3. Sa element** (holotype CPC 23114)[GB90-002/20] symmetrical element; **a,** right lateral view; **b,** left lateral view; **c,** posterior view; **d,** right lateral view showing basal cavity outline (× 115). **4. Sa element** (paratype CPC 23115)[GB90-002/6] symmetrical element; **a,** anterior view; **b,** right lateral view; **c,** left lateral view; **d,** left lateral view showing outline of basal cavity (× 140).

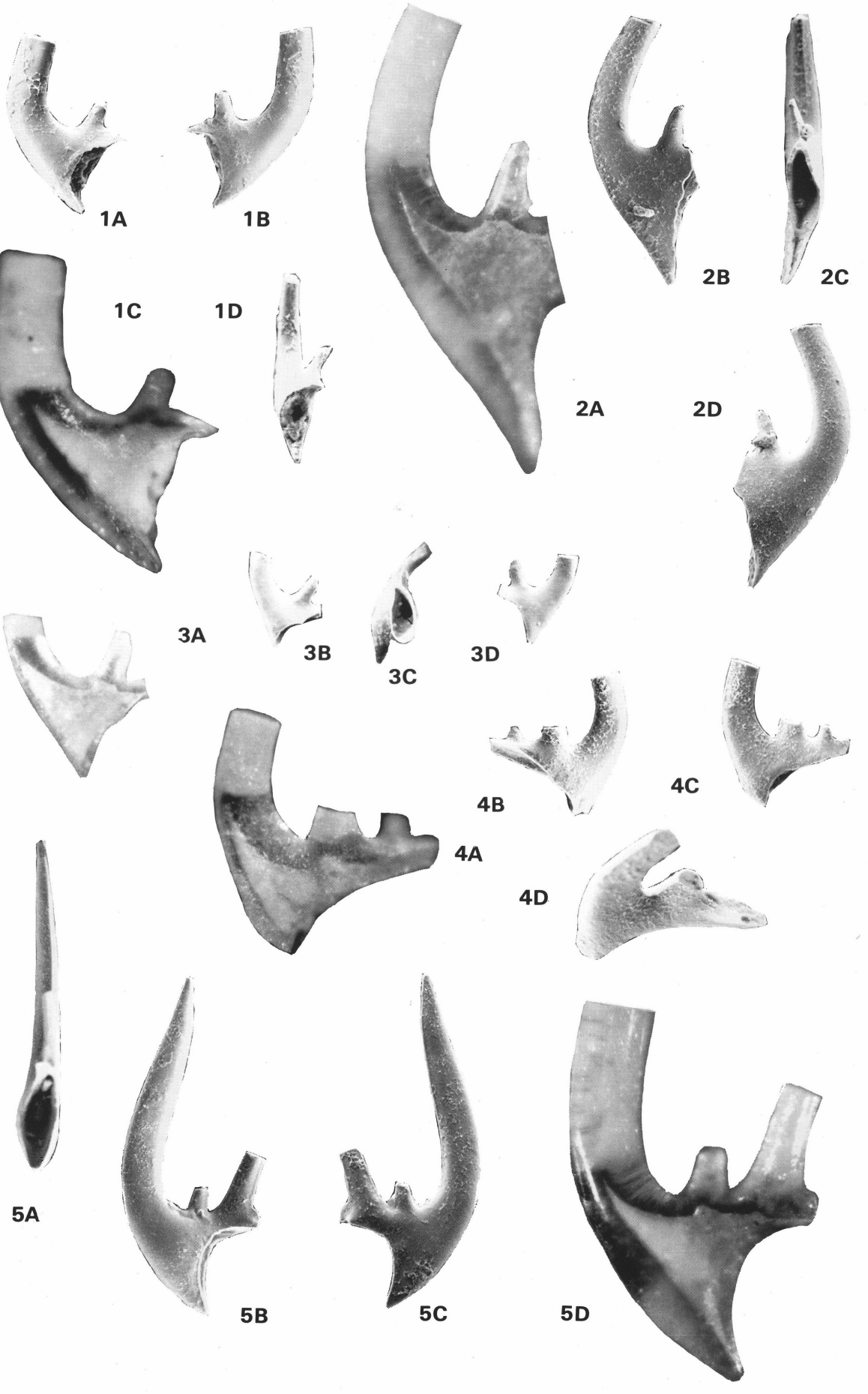
1A
1B
1C
1D
2A
2B
2C
2D
3A
3B
3C
3D
4A
4B
4C
4D
5A
5B
5C
5D

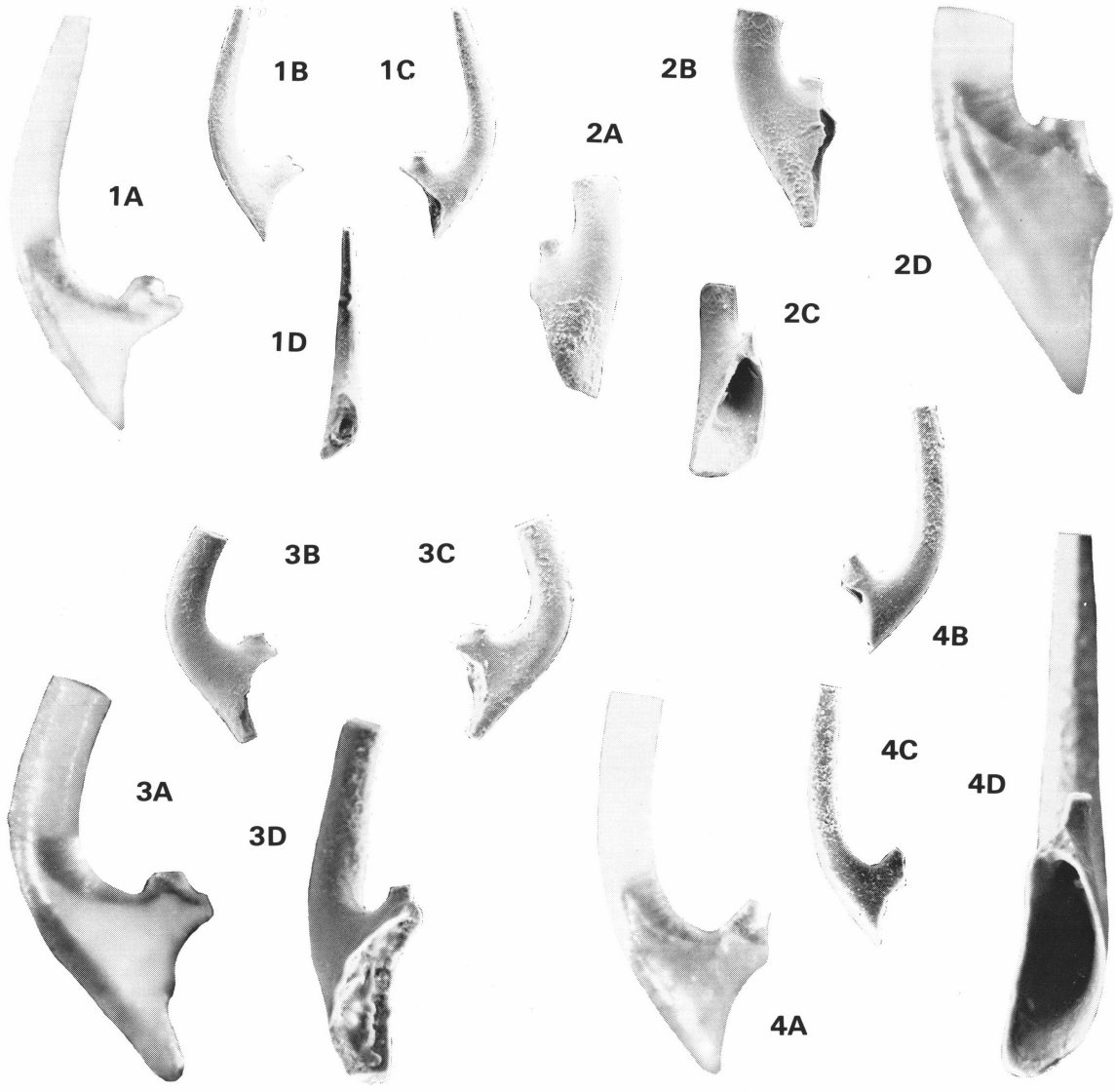

Figure 15. ***Cordylodus prolindstromi;*** **Sd elements.**
All figures ×70, except as noted.
1. Right element (paratype CPC 23121)[GB90-002/9]; **a,** inner lateral view showing basal cavity outline (×120); **b,** inner lateral view; **c,** outer lateral view; **d,** posterior view. **2. Right element** (paratype CPC 23122)[GB90-002/8]; **a,** outer lateral view; **b,** inner lateral view; **c,** posterior view; **d,** inner lateral view showing basal cavity outline (×125). **3. Left element** (paratype CPC 23123)[GB90-002/6]; **a,** outer lateral view showing basal cavity outline; **b,** outer lateral view; **c,** inner lateral view (×120); **d,** posterior view (×120). **4. Right element** (paratype CPC 23124)[GB90-002/3]; **a,** inner lateral view showing basal cavity outline (×125); **b,** outer lateral view; **c,** inner lateral view; **d,** posterior view (×195).

Figure 14 (facing page). ***Cordylodus prolindstromi;*** **Sc and Sb elements.**
All figures × 75, except as noted.
1. Sc element (paratype CPC 23116)[GB90-002/20] left element, ×65; **a,** outer lateral view; **b,** inner lateral view; **c,** outer lateral view showing basal cavity outline (×115); **d,** posterior view. **2. Sc element** (paratype CPC 23117)[GB90-002/20] right element, ×65; **a,** inner lateral view showing basal cavity outline (×120); **b,** inner lateral view; **c,** posterior view; **d,** outer lateral view. **3. Sb element** (paratype CPC 23118)[GB90-002/3] right element; **a,** inner lateral view showing outline of basal cavity (×135); **b,** inner lateral view; **c,** basal view; **d,** outer lateral view. **4. Sb element** (paratype CPC 23119)[GB90-002/6] right element; **a,** inner lateral view showing basal cavity outline (×130); **b,** outer lateral view; **c,** inner lateral view; **d,** oblique oral view. **5. Sb element** (paratype CPC 23120)[GB90-002/20] right element; **a,** posterior view; **b,** inner lateral view; **c,** outer lateral view; **d,** inner lateral view showing basal cavity outline (×130).

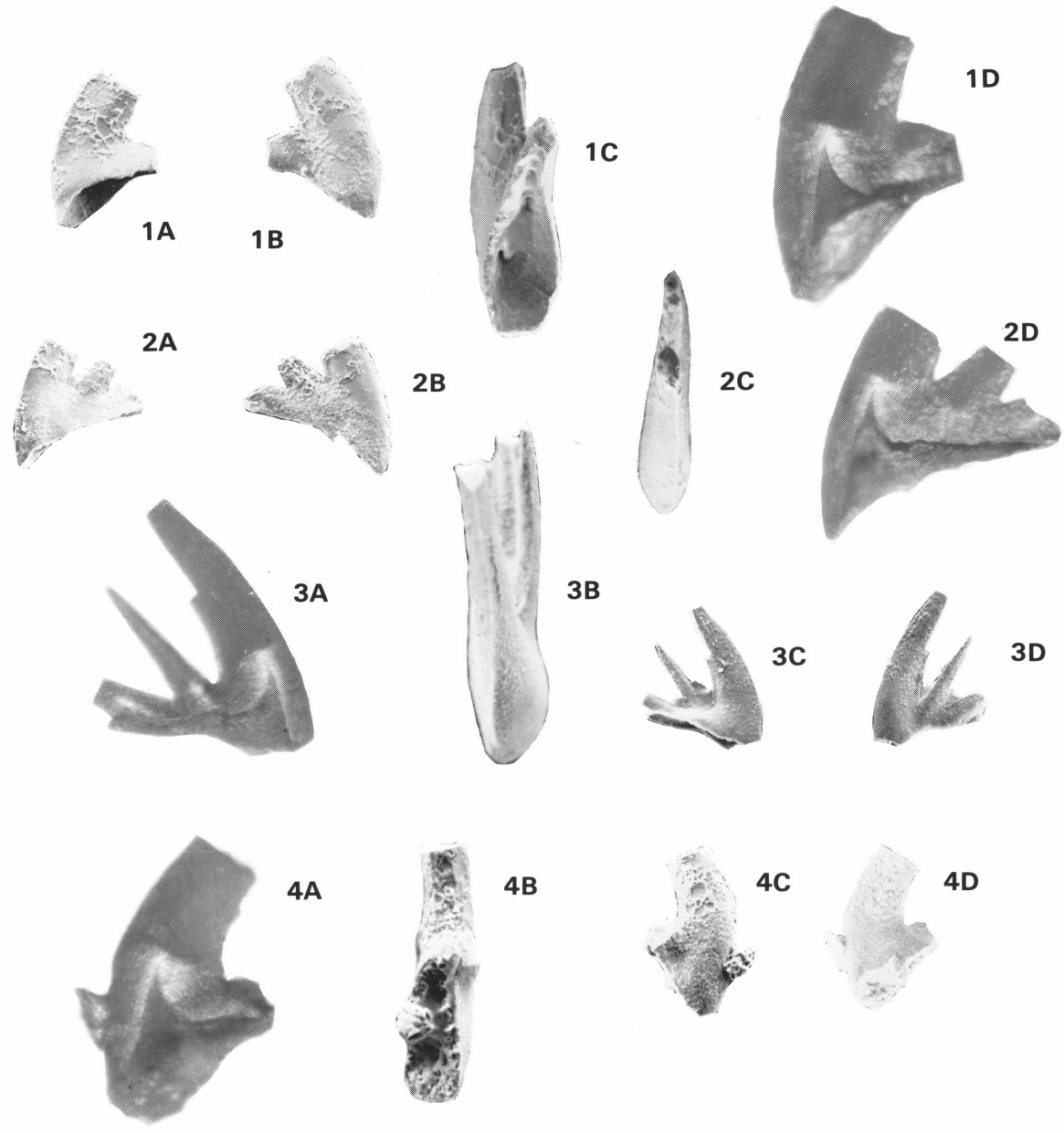

Figure 16. ***Cordylodus prolindstromi;*** **Pb and Pa elements.**
All figures × 70, except as noted.
1. Pb element (paratype CPC 23125)[GB90-002/3] right element; **a,** inner lateral view; **b,** outer lateral view; **c,** basal view (× 110); **d,** inner lateral view showing basal cavity outline (× 110). **2. Pb element** (paratype CPC 23126)[GB90-002/38] right element; **a,** inner lateral view; **b,** outer lateral view; **c,** oral view (× 125); **d,** inner lateral view showing basal cavity outline (× 125). **3. Pa element** (paratype CPC 23127)[GB90-002/6] left element; **a,** inner lateral view showing basal cavity outline (× 135); **b,** oral view (× 210); **c,** inner lateral view; **d,** outer lateral view. **4. Pa element** (paratype CPC 23128)[GB90-220/8] right element; **a,** inner lateral view showing basal cavity outline (× 110); **b,** basal view (110); **c,** outer lateral view; **d,** inner lateral view.

Locality information

The samples for this study were collected from the line of the Radke (1981) measured section of the Ninmaroo Formation on Black Mountain (Unbunmaroo). This corresponds approximately to the measured section of Druce & Jones (1971) at Black Mountain. For locality details see Druce & Jones (1971), Radke (1981) or Nicoll & Shergold (1991).

Acknowledgements

This paper was critically reviewed by Barry J. Cooper (South Australian Department of Industry, Trade and Technology) and Arne T. Nielsen (University of Copenhagen). Barry Cooper proposed the term biapical to describe the basal cavity with two apices. The author wishes to thank John Repetski for providing the Stora Backor sample and for discussions concerning matters raised by this investigation. Photography was the work of Arthur T. Wilson. Material illustrated is deposited in the Commonwealth Palaeontological Collection (CPC) at the Bureau of Mineral Resources, Canberra.

References

Andres, D., 1988 — Strukturen, apparate und phylogenie primitiver conodonten. *Palaeontographica Abteilung A,* 200, 105–152.

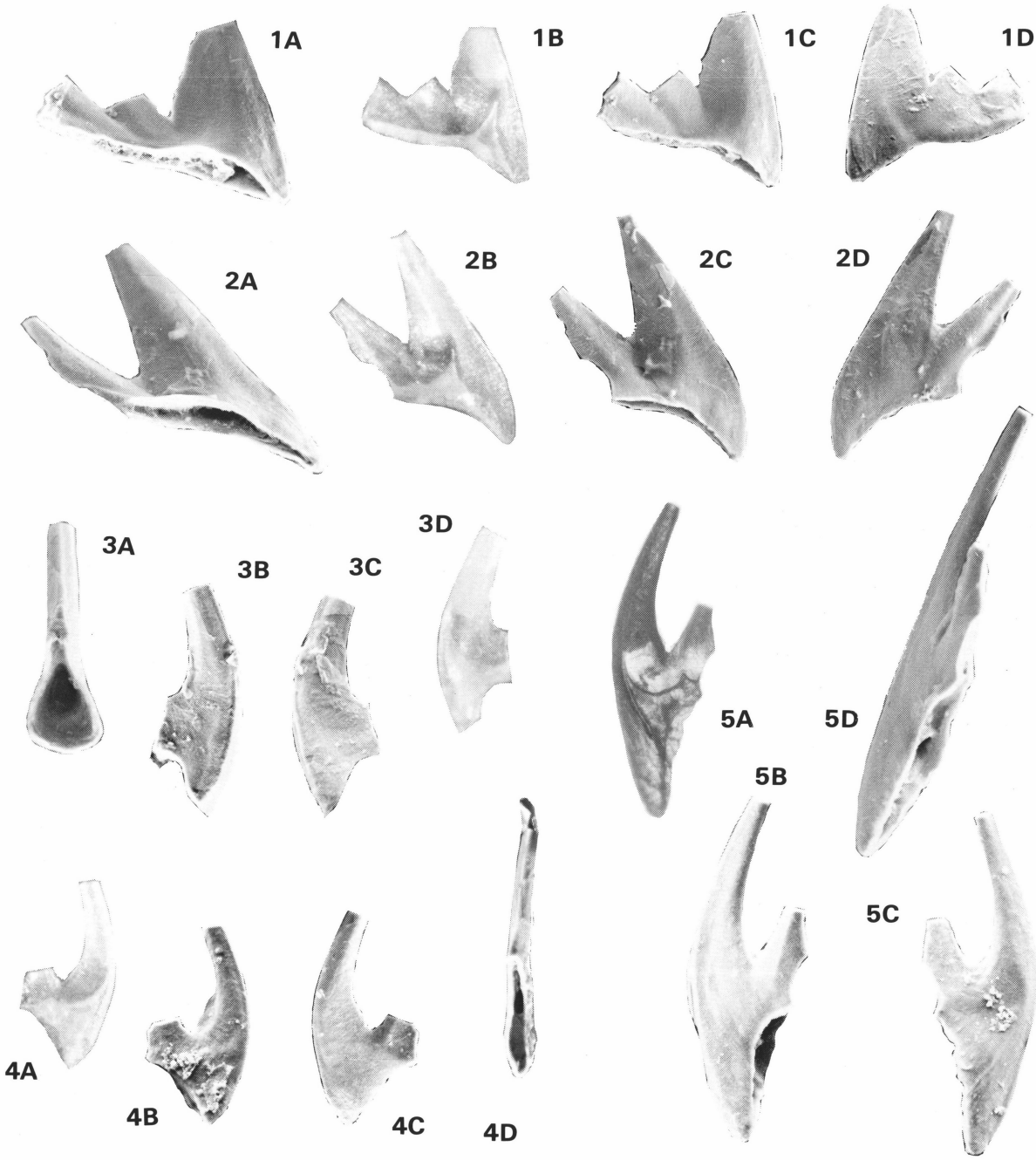

Figure 17. ***Cordylodus*** **sp. nov. B; M, Sa and Sc elements.**
All figures × 140, except as noted.
1. M element (CPC 23129)[GB90-002/96] left element; **a,** oblique posterior view (× 175); **b,** posterior lateral view showing basal cavity outline (× 120); **c,** posterior view; **d,** anterior view. **2. M element** (CPC 23130)[GB90-002/96] left element; **a,** oblique posterior view showing basal cavity outline (× 205); **b,** posterior view showing basal cavity outline (× 125); **c,** posterior view; **d,** anterior view. **3. Sa element** (CPC 23131)[GB90-002/96] symmetrical element; **a,** posterior view; **b,** right lateral view; **c,** left lateral view; **d,** left lateral view showing basal cavity outline (× 130). **4. Sc element** (CPC 23132)[GB90-002/96] left element; **a,** inner lateral view showing basal cavity outline (× 130); **b,** inner lateral view; **c,** outer lateral view; **d,** posterior view (× 170). **5. Sc element** (CPC 23133)[GB90-002/96] right element; **a,** inner lateral view showing basal cavity outline; **b,** inner lateral view; **c,** outer lateral view; **d,** oblique posterior view (× 190).

Bagnoli, G., Barnes, C.R. & Stevens, R.K., 1987 — Lower Ordovician (Tremadocian) conodonts from Broom Point and Green Point, western Newfoundland. *Bollettino della Societa Paleontologica Italiana,* 25, 145–158.

Barnes, C.R., 1988 — The proposed Cambrian–Ordovician global Boundary stratotype and point (GSSP) in Western Newfoundland, Canada. *Geological Magazine,* 125, 381–414.

Barnes, C.R. & Poplawski, M.L.S., 1973 — Lower and Middle Ordovician Conodonts from the Mystic Formation, Quebec, Canada. *Journal of Paleontology,* 47, 760–790.

Druce, E.C. & Jones, P.J., 1971 — Cambro-Ordovician conodonts from the Burke River Structural Belt, Queensland. *Bureau of Mineral Resources, Australia, Bulletin* 110, 1–159.

Ethington, R.L. & Clark, D.L., 1981 — Lower and Middle Ordovician Conodonts from the Ibex Area Western Millard Country, Utah. *Brigham Young University Geology Studies,* 28, 1–155.

Furnish, W.M., 1938 — Conodonts from the Prairie du Chien (Lower Ordovician) Beds of the upper Mississippi Valley. *Journal of Palaeontology,* 12, 318–340.

Hadding, A., 1913 — Under dicellograpusskiffern i Skåne jämte några

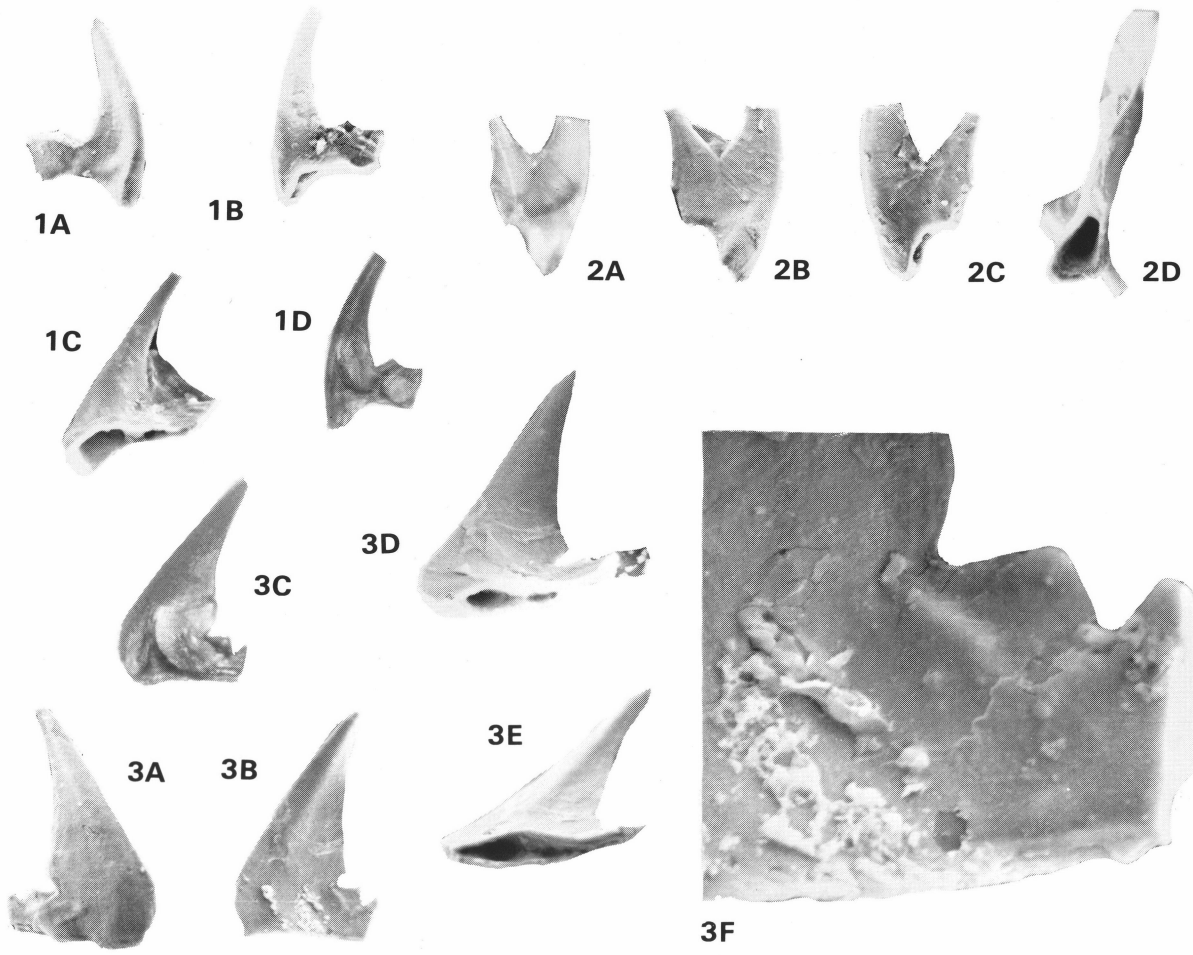

Figure 18. ***Cordylodus*** **sp. nov. B; S and P elements.**
All figures × 140, except as noted.
1. S (Sb or Sd) element (CPC 23134)[GB90-002/96] right element; **a,** outer lateral view; **b,** inner lateral view; **c,** oblique basal view (×170); **d,** inner lateral view showing basal cavity outline (×110). **2. S (Sb or Sd) element** (CPC 23135)[GB90-002/96] right element; **a,** outer lateral view showing basal cavity outline (×120); **b,** outer lateral view; **c,** inner lateral view; **d,** posterior view (×200). **3. P (Pb or Pa) element** (CPC 23136)[GB90-002/96] right element; **a,** outer lateral view; **b,** inner lateral view; **c,** inner lateral view showing basal cavity outline (×120); **d,** oblique lateral view (×220); **e,** oblique basal view (×220); **f,** enlargement of inner lateral view of posterior process showing compressed posterior process and denticles (×650).

därmed ekvivalenta bildningar. *Lunds Universitet Årsskrift Ny Foljd* 9, 90 pp.

Landing, E., Ludvigsen, R. & von Bitter, P.H., 1980. Upper Cambrian to Lower Ordovician conodont biostratigraphy and biofacies, Rabbitkettle Formation, District of Mackenzie. *Life Sciences Contributions Royal Ontario Museum,* 126, 1–42.

Lindström, M., 1955 — Conodonts from the lowermost Ordovician strata of south-central Sweden. *Geologiska Föreningens i Stockholm Förhandlingar,* 76, 517–614.

Miller, J.F., Taylor, M.E., Stitt, J.H., Ethington, R.L., Hintze, L.F. &Taylor, J.F., 1982 — Potential Cambrian-Ordovician boundary stratotype sections in the western United States. In Bassett, M.G. & Dean, W. T. (editors.). The Cambrian–Ordovician boundary: sections, fossils distributions and correlations. *National Museum of Wales, Geological Series* No. 3, 155–180.

Müller, K.J., 1959 — Kambrische conodonten. *Zeitschrift der Deutsche Geologische Gesellschaft,* III, 435–485.

Nicoll, R.S., 1990 — The genus *Cordylodus* and a latest Cambrian–earliest Ordovician conodont biostratigraphy. *BMR Journal of Australian Geology & Geophysics,* 11, 529–558.

Nicoll, R.S. & Shergold, J.H., 1991 — Revised Late Cambrian (pre-Payntonian-Datsonian) conodont biostratigraphy at Black Mountain, Georgina Basin, western Queensland, Australia. *BMR Journal of Australian Geology & Geophysics,* 12, 93–118.

Olgun, O., 1987 — Komponenten-analyse und conodonten-stratigraphie der Orthoceratenkalksteine im Gebiet Falbygden, Västergötland, Mittelschweden. *Sveriges geologiska undersökining, Ser. Ca,* 70, 1–79.

Pander, C.H., 1856 — Monographie der fossilen fische des Silurischen Systems der Russich–Baltischen gouvernements. *Akademie der Wissenschaften, St. Petersburg,* 91 pp.

Radke, B.M., 1981 — Lithostratigraphy of the Ninmaroo Formation (Upper Cambrian–Lower Ordovician), Georgina Basin, Queensland and Northern Territory. *Bureau of Mineral Resources, Australia, Report* 181.

Ripperdan, R.L., Kirschvink, J.L., Apollonov, M.K., Ma, G.G. & Zhang, Z.C., 1990 — Magnetostratigraphy of the Cambrian–Ordovician boundary interval. *Paper distributed at the 3rd International Symposium on the Cambrian System, Novosibirsk, August 1990,* 106 pp.

Shergold, J.H. & Nicoll, R.S. (in press) — Revised Cambrian–Ordovician boundary biostratigraphy, Black Mountain, western Queensland. *Balkema, Rotterdam.*